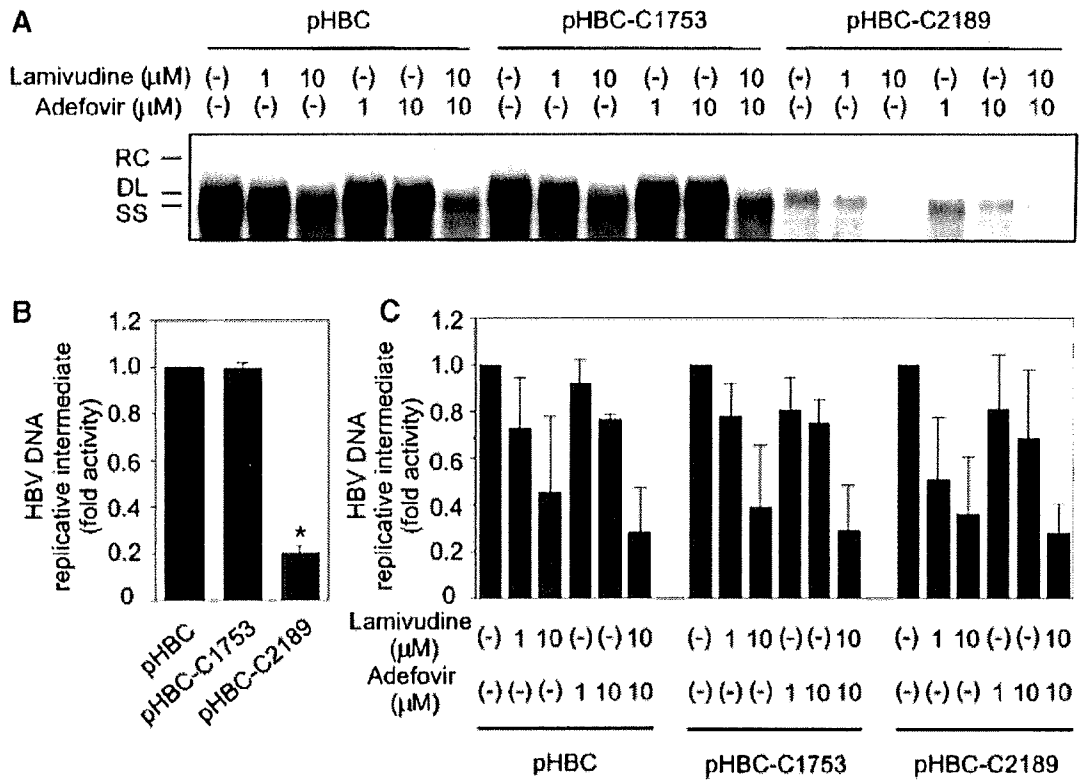

Fig. 3. In vitro transfection analysis to examine viral replicative competence and susceptibility to the treatment with lamivudine and/or adefovir. Huh-7 cells were transfected with pHBC, pHBC-C1753 and pHBC-C2189, and treated with lamivudine alone, adefovir alone, lamivudine plus adefovir, or left untreated. The HBV DNA replicative intermediate in the cytoplasmic fraction of the cells was detected by Southern blot analysis. A: Representative result of Southern blot analysis to detect the HBV DNA replicative intermediate. SS, single-stranded HBV DNA. DL, double-stranded linear HBV DNA. RC, relaxed circular HBV DNA. B: Quantitative analysis of the HBV DNA replicative intermediate in cells transfected with pHBC, pHBC-C1753 and pHBC-C2189 without nucleos(t)ide analog treatment. The level of the HBV DNA replicative intermediate in the case of transfection with pHBC was considered as 1, and its fold activity in the case of transfection with the mutant HBV-expressing plasmid was calculated. The experiment was done three times, and the results are presented as the mean ± SD. $^*P < 0.001$ versus pHBC and pHBC-C1753 groups. C: Degree of reduction in the HBV DNA replicative intermediate after treatment with lamivudine and/or adefovir in cells transfected with pHBC, pHBC-C1753 and pHBC-C2189. The level of the HBV DNA replicative intermediate in untreated cells was considered as 1, and its fold activity in cells treated with lamivudine and/or adefovir was calculated. The experiment was done three times, and the results are presented as the mean ± SD.

regimen for lamivudine-resistant patients with type B chronic hepatitis. In the present study, the viral mutations associated with the effect of this regimen were investigated by screening the whole HBV genome via sequencing analysis of full-length viral DNA. Two mutations, V1753 and C2189, were identified as significant determinants of the therapeutic efficacy. Using adefovir dipivoxil added to lamivudine treatment, HBV DNA tended to decline to the undetectable level more frequently in patients with the V1753 or C2189 mutation than in those without it. In univariate analysis, only the presence of the V1753 or C2189 mutation was shown to be a factor contributing to sustained clearance of HBV DNA during adefovir dipivoxil therapy. Multivariate analysis also revealed that the V1753 and C2189 mutations, as well as high ALT and low HBV DNA at baseline, were independent factors associated with a better antiviral effect. Reports from the United States and European countries have revealed that female gender, high ALT, low viral load, absence of HBeAg and genotype D rather than genotype A were related to a better outcome of adefovir dipivoxil therapy in nucleoside-naïve and lamivudine-resistant patients with type B chronic hepatitis [Lampertico et al., 2005; Fung et al., 2006; Buti et al., 2007]. The findings of the present study from Japan, a genotype C HBV-endemic area, agreed in part with these reports. Of particular interest is the finding that the therapeutic efficacy of adefovir dipivoxil added to lamivudine may be affected not only by clinical factors but also the genomic background of HBV such as the presence of the V1753 or C2189 mutation in lamivudine-resistant patients with type B chronic hepatitis. In addition, serial sequencing analysis revealed that both the V1753 and C2189 mutations tended to be selected during lamivudine therapy associated with the establishment of lamivudine resistance, although they have been shown to be mutations which occur naturally during the course of HBV infection [Ehata et al., 1991; Bozkaya et al., 1996; Takahashi et al., 1999; Imamura et al., 2003; Ozasa et al., 2006; Tanaka et al., 2006].

The findings of the present study suggest higher sensitivity to adefovir dipivoxil therapy of the V1753 and C2189 mutant viruses compared to the wild-type virus in vivo. However, in vitro transfection analysis showed no differences in susceptibility to adefovir, as well as to lamivudine, among the wild-type virus and the C1753 and C2189 mutant viruses. This indicates that the V1753 and C2189 mutant viruses may be eradicated more efficiently by adefovir dipivoxil therapy than the wild-type virus regardless of a direct antiviral effect of adefovir dipivoxil. The V1753 and C2189 mutant viruses may induce stronger immune responses against the viral pathogens than the wild-type virus, which might result in more frequent viral eradication under adefovir dipivoxil therapy in patients having the V1753 or C2189 mutant virus compared to those with the wild-type virus.

Of the 1421 HBV strains, whose nucleotide sequences of the BCP, precore and core regions had been identified and registered in the Hepatitis Virus Database (http://s2as02.genes.nig.ac.jp), there were 259 (18%) strains with the V1753 mutation and 127 (9%) strains with the C2189 mutation. The V1753 mutation was found in strains of all HBV genotypes, whereas the C2189 mutation was found in strains of genotypes A, B, C, and E. Thus, the V1753 and C2189 mutations were not specific for genotype C but common in other HBV genotypes.

The V1753 mutation occurring in the BCP not only influences the core promoter activity but also causes the I127T/N/S amino acid change of the overlapping X gene. This mutation has been detected in a considerable proportion of chronic HBV carriers, especially coupled with the adjacent T1762/A1764 mutation [Kidd-Ljunggren et al., 1997; Takahashi et al., 1999]. Indeed, all 11 patients with the V1753 mutation possessed the T1762/A1764 mutation in the current study. It has also been shown that, among patients with type B chronic hepatitis of genotype C, the V1753 mutation was found more frequently in patients with HCC than in those without it [Tanaka et al., 2006]. In acute HBV infection, the frequency of mutation has been reported to be higher in patients with fulminant hepatitis than in those with non-fulminant hepatitis [Imamura et al., 2003; Ozasa et al., 2006]. In vitro transfection assay revealed that the C1753 mutant virus possessed similar replicative competence to the wild-type virus, though viruses having the G1753 and A1753 mutation were not examined. Also, the in vitro replicative competence did not differ between the wild-type and C1753 mutant viruses when the T1762/A1764 mutation was introduced into the backbone HBV structure (data not shown). According to these observations, the serious disease course and better response to adefovir dipivoxil therapy caused by the V1753 mutation, as suggested by the present study and other previous investigations [Imamura et al., 2003; Ozasa et al., 2006; Tanaka et al., 2006], may not be due to the modification of the viral replicative competence. Further studies should be done to clarify why the V1753 mutation is involved in the active liver disease and the better outcome of adefovir dipivoxil therapy in patients with HBV infection.

The C2189 mutation, which leads to the I97L amino acid change in the core gene, has also been shown to be detected frequently in patients with type B chronic hepatitis [Ehata et al., 1991; Bozkaya et al., 1996], although the relevance of the mutation to a particular disease course has not been elucidated fully. Previous in vitro transfection studies have suggested that the virus with the C2189 mutation resulted in excessive secretion of the immature virion and enhanced viral replication [Yuan et al., 1999; Suk et al., 2002]. This does not agree with the present result showing lower replicative competence of the C2189 mutant virus than the wild-type virus. This discrepancy may be due to the usage of HBV-expressing plasmids of different viral strains. The virological and clinical significance of the C2189 mutant virus should be assessed by further detailed investigation.

In summary, the results of the present study indicate that the presence of the two viral mutations, V1753 and C2189, may be associated with a better therapeutic effect of adefovir dipivoxil added to lamivudine based on the results of screening of the full-length HBV genome obtained from lamivudine-resistant patients with type B chronic hepatitis. As the present study examined a limited number of patients with HBV of genotype C, further studies with a larger number of patients with different genotypes should lead to a better understanding of how identifying these mutations can be useful in a clinical setting.

REFERENCES

Bozkaya H, Ayola B, Lok AS. 1996. High rate of mutations in the hepatitis B core gene during the immune clearance phase of chronic hepatitis B virus infection. Hepatology 24:32–37.

Buti M, Elefsiniotis I, Jardi R, Vargas V, Rodriguez-Frias F, Schapper M, Bonovas S, Esteban R. 2007. Viral genotype and baseline load predict the response to adefovir treatment in lamivudine-resistant chronic hepatitis B patients. J Hepatol 47:366–372.

Carman WF, Jacyna MR, Hadziyannis S, Karayiannis P, McGarvey MJ, Makris A, Thomas HC. 1989. Mutation preventing formation of hepatitis B e antigen in patients with chronic hepatitis B infection. Lancet 2:588–591.

Dienstag JL, Schiff ER, Wright TL, Perrillo RP, Hann HW, Goodman Z, Crowther L, Condreay LD, Woessner M, Rubin M, Brown NA. 1999. Lamivudine as initial treatment for chronic hepatitis B in the United States. N Engl J Med 341:1256–1263.

Ehata T, Omata M, Yokosuka O, Hosoda K, Ohto M. 1991. Variations in codons 84-101 in the core nucleotide sequence correlate with hepatocellular injury in chronic hepatitis B virus infection. J Clin Invest 89:332–338.

Fujiyama A, Miyanohara A, Nozaki C, Yoneyama T, Ohtomo N, Matsubara K. 1983. Cloning and structural analyses of hepatitis B virus DNAs, subtype adr. Nucleic Acids Res 11:4601–4610.

Fung SK, Chae HB, Fontana RJ, Conjeevaram H, Marrero J, Oberhelman K, Hussain M, Lok AS. 2006. Virologic response and resistance to adefovir in patients with chronic hepatitis B. J Hepatol 44:283–290.

Hadziyannis SJ, Tassopoulos NC, Heathcote EJ, Chang TT, Kitis G, Rizzetto M, Marcellin P, Lim SG, Goodman Z, Wulfsohn MS, Xiong S, Fry J, Brosgart CL, Adefovir Dipivoxil 438 Study Group. 2003. Adefovir dipivoxil for the treatment of hepatitis B e antigen-negative chronic hepatitis B. N Engl J Med 348:800–807.

Hadziyannis SJ, Tassopoulos NC, Heathcote EJ, Chang TT, Kitis G, Rizzetto M, Marcellin P, Lim SG, Goodman Z, Ma J, Arterburn S, Xiong S, Currie G, Brosgart CL, Adefovir Dipivoxil 438 Study

Group. 2005. Long-term therapy with adefovir dipivoxil for HBeAg-negative chronic hepatitis B. N Engl J Med 352:2673–2681.

Hadziyannis SJ, Tassopoulos NC, Heathcote EJ, Chang TT, Kitis G, Rizzetto M, Marcellin P, Lim SG, Goodman Z, Ma J, Brosgart CL, Borroto-Esoda K, Arterburn S, Chuck SL, Adefovir Dipivoxil 438 Study Group. 2006. Long-term therapy with adefovir dipivoxil for HBeAg-negative chronic hepatitis B for up to 5 years. Gastroenterology 131:1743–1751.

Imamura T, Yokosuka O, Kurihara T, Kanda T, Fukai K, Imazeki F, Saisho H. 2003. Distribution of hepatitis B viral genotypes and mutations in the core promoter and precore regions in acute forms of liver disease in patients from Chiba, Japan. Gut 52:1630–1637.

Kanada A, Takehara T, Ohkawa K, Tatsumi T, Sakamori R, Yamaguchi S, Uemura A, Kohga K, Sasakawa A, Hikita H, Hijioka T, Katayama K, Deguchi M, Kagita M, Kanto T, Hiramatsu N, Hayashi N. 2007. Type B fulminant hepatitis is closely associated with a highly mutated hepatitis B virus strain. Intervirology 50:394–401.

Karatayli E, Karayalçin S, Karaaslan H, Kayhan H, Türkyilmaz AR, Sahin F, Yurdaydin C, Bozdayi AM. 2007. A novel mutation pattern emerging during lamivudine treatment shows cross-resistance to adefovir dipivoxil treatment. Antivir Ther 12:761–768.

Kidd-Ljunggren K, Oberg M, Kidd AH. 1997. Hepatitis B virus X gene 1751 to 1764 mutations: Implications for HBeAg status and disease. J Gen Virol 78:1469–1478.

Lai CL, Chien RN, Leung NW, Chang TT, Guan R, Tai DI, Ng KY, Wu PC, Dent JC, Barber J, Stephenson SL, Gray DF. 1998. A one-year trial of lamivudine for chronic hepatitis B. Asia Hepatitis Lamivudine Study Group. N Engl J Med 339:61–68.

Lai CL, Dienstag J, Schiff E, Leung NW, Atkins M, Hunt C, Brown N, Woessner M, Boehme R, Condreay L. 2003. Prevalence and clinical correlates of YMDD variants during lamivudine therapy for patients with chronic hepatitis B. Clin Infect Dis 36:687–696.

Lampertico P, Vigano M, Manenti E, Iavarone M, Lunghi G, Colombo M. 2005. Adefovir dipivoxil suppresses hepatitis B in HBeAg-negative patients developing genotypic resistance to lamivudine. Hepatology 42:1414–1419.

Lee YS, Suh DJ, Lim YS, Jung SW, Kim KM, Lee HC, Chung YH, Lee YS, Yoo W, Kim SO. 2006. Increased risk of adefovir resistance in patients with lamivudine-resistant chronic hepatitis B after 48 weeks of adefovir dipivoxil monotherapy. Hepatology 43:1385–1391.

Leung NW, Lai CL, Chang TT, Guan R, Lee CM, Ng KY, Lim SG, Wu PC, Dent JC, Edmundson S, Condreay LD, Chien RN, On behalf of the Asia Hepatitis Lamivudine Study Group. 2001. Extended lamivudine treatment in patients with chronic hepatitis B enhances hepatitis B e antigen seroconversion rates: Results after 3 years of therapy. Hepatology 33:1527–1532.

Liaw YF, Leung NW, Chang TT, Guan R, Tai DI, Ng KY, Chien RN, Dent J, Roman L, Edmundson S, Lai CL. 2000. Effects of extended lamivudine therapy in Asian patients with chronic hepatitis B. Asia Hepatitis Lamivudine Study Group. Gastroenterology 119:172–180.

Marcellin P, Chang TT, Lim SG, Tong MJ, Sievert W, Shiffman ML, Jeffers L, Goodman Z, Wulfsohn MS, Xiong S, Fry J, Brosgart CL, Adefovir Dipivoxil 437 Study Group. 2003. Adefovir dipivoxil for the treatment of hepatitis B e antigen-positive chronic hepatitis B. N Engl J Med 348:808–816.

Ohkawa K, Takehara T, Kato M, Deguchi M, Kagita M, Hikita H, Sasakawa A, Kohga K, Uemura A, Sakamori R, Yamaguchi S, Miyagi T, Ishida H, Tatsumi T, Hayashi N. 2008. Supportive role played by precore and preS2 genomic changes on establishment of lamivudine-resistant hepatitis B virus. J Infect Dis 198:1150–1158.

Okamoto H, Tsuda F, Akahane Y, Sugai Y, Yoshiba M, Moriyama K, Tanaka T, Miyakawa Y, Mayumi M. 1994. Hepatitis B virus with mutations in the core promoter for an e antigen-negative phenotype in carriers with antibody to e antigen. J Virol 68:8102–8110.

Ozasa A, Tanaka Y, Orito E, Sugiyama M, Kang JH, Hige S, Kuramitsu T, Suzuki K, Tanaka E, Okada S, Tokita H, Asahina Y, Inoue K, Kakumu S, Okanoue T, Murawaki Y, Hino K, Onji M, Yatsuhashi H, Sakugawa H, Miyakawa Y, Ueda R, Mizokami M. 2006. Influence of genotypes and precore mutations on fulminant or chronic outcome of acute hepatitis B virus infection. Hepatology 44:326–334.

Perrillo R, Hann HW, Mutimer D, Willems B, Leung N, Lee WM, Moorat A, Gardner S, Woessner M, Bourne E, Brosgart CL, Schiff E. 2004. Adefovir dipivoxil added to ongoing lamivudine in chronic hepatitis B with YMDD mutant hepatitis B virus. Gastroenterology 126:81–90.

Peters MG, Hann Hw H, Martin P, Heathcote EJ, Buggisch P, Rubin R, Bourliere M, Kowdley K, Trepo C, Gray Df D, Sullivan M, Kleber K, Ebrahimi R, Xiong S, Brosgart CL. 2004. Adefovir dipivoxil alone or in combination with lamivudine in patients with lamivudine-resistant chronic hepatitis B. Gastroenterology 126:91–101.

Suk FM, Lin MH, Newman M, Pan S, Chen SH, Liu JD, Shih C. 2002. Replication advantage and host factor-independent phenotypes attributable to a common naturally occurring capsid mutation (I97L) in human hepatitis B virus. J Virol 76:12069–12077.

Takahashi K, Ohta Y, Kanai K, Akahane Y, Iwasa Y, Hino K, Ohno N, Yoshizawa H, Mishiro S. 1999. Clinical implications of mutations C-to-T1653 and T-to-C/A/G1753 of hepatitis B virus genotype C genome in chronic liver disease. Arch Virol 144:1299–1308.

Tanaka Y, Mukaide M, Orito E, Yuen MF, Ito K, Kurbanov F, Sugauchi F, Asahina Y, Izumi N, Kato M, Lai CL, Ueda R, Mizokami M. 2006. Specific mutations in enhancer II/core promoter of hepatitis B virus subgenotypes C1/C2 increase the risk of hepatocellular carcinoma. J Hepatol 45:646–653.

Villet S, Pichoud C, Villeneuve JP, Trepo C, Zoulim F. 2006. Selection of a multiple drug-resistant hepatitis B virus strain in a liver-transplanted patient. Gastroenterology 131:1253–1261.

Yuan TT, Tai PC, Shih C. 1999. Subtype-independent immature secretion and subtype-dependent replication deficiency of a highly frequent, naturally occurring mutation of human hepatitis B virus core antigen. J Virol 73:10122–10128.

Yuh CH, Chang YL, Ting LP. 1992. Transcriptional regulation of precore and pregenomic RNAs of hepatitis B virus. J Virol 66:4073–4084.

J Gastroenterol (2009) 44:889–896
DOI 10.1007/s00535-009-0081-3

ORIGINAL ARTICLE—ALIMENTARY TRACT

A novel therapeutic strategy with anti-CD9 antibody in gastric cancers

Taisei Nakamoto · Yoko Murayama · Kenji Oritani · Claude Boucheix · Eric Rubinstein · Makoto Nishida · Fumie Katsube · Kenji Watabe · Shinichi Kiso · Shusaku Tsutsui · Shinji Tamura · Yasuhisa Shinomura · Norio Hayashi

Received: 8 January 2009 / Accepted: 5 April 2009 / Published online: 26 May 2009

Abstract

Background CD9 is a member of the tetraspanins, and has been shown to be involved in a variety of cellular activities such as motility, cell signaling, proliferation, adhesion, and metastasis. However, very little is known about the involvement of CD9 in the process of development of primary tumors. In the present study, we investigated whether anti-CD9 monoclonal antibody (ALB6) has antitumor effects in human gastric cancer cell xenografts.

Methods Human gastric cancer cell lines (MKN-28) (5×10^6 cells/animal) were inoculated subcutaneously into the dorsal region of SCID mice (five mice in each group). After a tumor was visualized, animals were assigned to either the ALB6 treatment group or the control IgG treatment group (100 μg/body/time, intravenous, three times per week. Day 1, 4, and 7 of first week). Then tumor volumes were monitored every day. Proliferation of tumor was analyzed by 5-bromo-2′-deoxyuridine (BrdU) immunostaining, apoptosis was determined by terminal deoxynucleotidyl transferase-mediated dUTP-biotin nick-end labeling (TUNEL) methods, and angiogenesis was assessed by counting the number of CD34-positive endothelial cells.

Results Tumor volume was significantly suppressed ($1{,}682 \pm 683$ mm^3 versus $4{,}507 \pm 1{,}012$ mm^3; $P = 0.049$), the BrdU labeling indexes were significantly decreased ($10.9 \pm 1.1\%$ versus $17.2 \pm 1.4\%$; $P = 0.009$), the apoptotic indexes were significantly increased ($1.98 \pm 0.48\%$ versus $0.72 \pm 0.09\%$; $P = 0.034$), and tumor microvessel densities were significantly suppressed ($671{,}922 \pm 34{,}505$ pixels/mm^2 versus $1{,}135{,}043 \pm 36{,}086$ pixels/mm^2; $P = 0.037$) in the ALB6 treatment group compared with the control IgG treatment group.

Conclusions These results suggest that administration of anti-CD9 antibody to mice bearing human gastric cancer cells successfully inhibits tumor progression via antiproliferative, proapoptotic, and antiangiogenetic effects.

T. Nakamoto · K. Watabe · S. Kiso · S. Tsutsui · N. Hayashi
Department of Gastroenterology and Hepatology,
Graduate School of Medicine,
Osaka University, Suita, Japan

Y. Murayama (✉)
Department of Gastroenterology and Hepatology,
Itami City Hospital, Koyaike 1-100, Itami, Japan
e-mail: murayama@hosp.itami.hyogo.jp;
yokom@imed2.med.osaka-u.ac.jp

K. Oritani
Department of Hematology/Oncology,
Graduate School of Medicine,
Osaka University, Suita, Japan

C. Boucheix · E. Rubinstein
Institut National de la Santé et de la Recherche Medicale,
Unité 554, Montpellier, France

M. Nishida
Health Care Center,
Osaka University, Toyonaka, Japan

F. Katsube
Department of Metabolic Medicine,
Graduate School of Medicine,
Osaka University, Suita, Japan

S. Tamura
Department of Internal Medicine,
Minoh City Hospital, Minoh, Japan

Y. Shinomura
First Department of Internal Medicine,
Sapporo Medical University, Sapporo, Japan

Keywords CD9 · Tetraspanin · Proliferation · Tumorigenicity

Abbreviations

BrdU	5-Bromo-2′-deoxyuridine
JNK/SAPK	c-Jun NH_2-terminal kinase/stress-activated protein kinase
MAPK	Mitogen-activated-protein kinase
TUNEL	Terminal deoxynucleotidyl transferase-mediated dUTP-biotin nick-end labeling
ABC	Avidin–biotin peroxidase complex
DAB	3,3′-Diaminobenzidine tetrahydrochloride
FCS	Fetal calf serum
PBS	Phosphate-buffered saline
EGFR	Epidermal growth factor receptor
SEM	Standard error of the mean
cDNA	complementary Deoxyribonucleic acid

Introduction

Gastric cancer is one of the most common malignancies. The World Health Organization estimates that stomach cancer is the second most common (10.4%) cause of death from cancer, with annual deaths of almost 1,000,000 [1]. The 5-year survival rate remains less than 30% in patients with gastric cancer in the USA [2]. Although various treatment modalities have been developed to treat this disorder, many of them have failed to provide complete reduction of gastric carcinoma in patients [3].

Tetraspanins have four putative membrane-spanning domains, short N- and C-terminal cytoplasmic domains, a small intracellular loop, and two extracellular loops [4–6]. Members of this family are involved in many physiological and pathological processes such as fertilization, cellular adhesion, motility, and tumor invasion [4–7]. Tetraspanins can act as molecular facilitators or adaptors, which organize a network of interactions among the cell surface molecules, known as the "tetraspanin web" or tetraspan-enriched microdomains [7, 8].

The CD9 protein is a member of the tetraspanin family and has been identified as a suppressor of cancer spread [9]. Several clinical studies have also shown an important prognostic value in which reduced MRP-1/CD9 expression is associated with poor prognosis in various cancers, including non-small-cell lung cancers [10], breast cancers [11], colon cancers [12], pancreatic cancers [13], and ovarian carcinomas [14]. The expression of CD9 is closely related to metastasis of gastrointestinal carcinomas. For example, reduced CD9 expression is significantly associated with venous vessel invasion and liver metastasis in patients with colon cancers [12, 15]. The amount of CD9 is inversely correlated to lymph node status in gastric cancers and in esophageal squamous cell carcinomas [16, 17]. Therefore, these findings strongly suggest that CD9 plays indispensable roles in the progression of malignant tumors [10–15]. Moreover, CD9 is highly expressed in gastrointestinal carcinomas (Table 1). Thus, CD9 might be considered as a potential biomarker of these malignancies.

We previously reported one possible mechanism in which the treatment of gastrointestinal cancer cell lines with anti-CD9 antibody induced apoptosis via the selective activation of c-Jun NH_2-terminal kinase/stress-activated protein kinase (JNK/SAPK), p38 mitogen-activated-protein kinase (MAPK), caspase-3, and the p46 Shc isoform [19]. Thus, CD9 associates with not only intra-signaling molecules but also integrins, a proform of HB-EGF, and co-receptor molecules. Moreover, we recently reported that CD9 enhances the internalization of EGFR and reduces EGF-EGFR-induced signals, which mediate proliferation and survival of gastrointestinal cancer cells [20]. However, very little is known about the involvement of CD9 in the process of development of primary tumors. In the present study, we investigated the antitumor activity of anti-CD9 antibody ALB6 in vivo in a mouse xenograft model of human gastric cancer.

Materials and methods

Reagents and antibodies

An anti-human CD9 monoclonal antibody (mAb), ALB6, was purchased from MBL (Nagoya, Japan). The control purified mouse IgG1 (MOPC-21) and 5-bromo-2′-deoxyuridine (BrdU) for the injection were purchased from Sigma–Aldrich (Tokyo, Japan), and anti-BrdU mAb for the immunohistochemistry was purchased from GE Healthcare Bio-Sciences (Tokyo, Japan). The anti-CD34 mAb was purchased from Cedarlane (Hornby, Ontario, Canada).

Cell culture

The human gastric cancer cell line, MKN-28 (#JCRB-0253), was supplied by the Japanese Cancer Research Bank (Tokyo, Japan). The cells were cultured in RPMI 1640

Table 1 CD9 expression in gastrointestinal cancer

	CD9 positive/cases (%)	Author	Reference
Gastric cancer	26/36 (72.2)	Murayama	[17]
	45/78 (57.7)	Hori	[18]
Colon cancer	56/82 (68.3)	Mori	[12]
Pancreatic cancer	18/40 (45)	Sho	[13]

medium (Gibco BRL, Grand Island, NY, USA) supplemented with 10% heat-inactivated fetal calf serum (FCS; Whittaker Bioproducts, Walkersville, MD, USA), 100 units/ml penicillin, and 100 μg/ml streptomycin in a humidified atmosphere of 5% CO_2 and 95% air at 37°C.

Xenograft analysis

Animal experiments were performed according to the guidelines of the Committee on Experimental Animals of Osaka University. We purchased 30 female athymic mice (BALB/c nu/nu; 5 weeks old; 18–22 g) from CLEA JAPAN, Inc. (Tokyo, Japan). The animals were maintained under specific pathogen-free conditions using a laminar airflow rack and had continuous free access to sterilized food (gamma-ray-irradiated food, CL-2; CLEA JAPAN) and autoclaved water. Experiments were started after more than 1 week of acclimatization.

Each mouse was inoculated with MKN-28 cells (5×10^6 cells/animal) subcutaneously on the left side of the back on day 1. The cell viability of the injected MKN-28 cells was more than 90%. Nine days thereafter, the xenografts were identifiable as a mass of more than 6 mm in maximal diameter in all recipients. The animals were randomly assigned to two groups. The ALB6 group was injected intravenously at 100 μg/body/time of ALB6, three times at 3-day intervals for a week. The control group was injected at 100 μg/body/time of nonimmunized IgG1, three times at 3-day intervals for a week, and tumorigenesis was monitored every day. Tumor size was measured daily and tumor volumes (mm^3) from each group were assessed using the formula width^2 × length × 0.52 (mm^3) according to a previously published method [21].

Histopathological and immunohistochemical examinations

To examine the mitotic activity, on the 36th day, mice were intraperitoneally injected with BrdU (10 mg/ml; 100 mg/kg body weight). Six hours after injection of BrdU, each mouse was anesthetized with pentobarbital (Schering-plough, Tokyo Japan). All tumors were dissected from the body and divided along the longest diameter with a surgical knife.

Half of each specimen was embedded in a cryocompound (Tissue-Tek OCT-compound; Sakura Finetech, Tokyo, Japan), and immediately immersed in liquid nitrogen. The other half of each specimen was fixed in 10% phosphate-buffered formalin, embedded in paraffin, and sectioned at a thickness of 4 μm. The sections were deparaffinized and gradually hydrated, and examined by histology of hematoxylin and eosin (H&E) staining, BrdU immunostaining, terminal deoxynucleotidyl transferase-mediated dUTP-biotin nick-end labeling (TUNEL) assay, and immunohistochemical staining of CD34. The sections were observed by microscope (PROVIS Ax 80 TR; Olympus, Tokyo, Japan).

Proliferation analysis

Specimens were deparaffinized and incubated with a primary antibody against BrdU (1:100). The specimens were treated with the peroxidase anti-mouse IgG 2a, followed by an avidin–biotin peroxidase complex (ABC) method using a Vecstatin kit (Vector Laboratories, Burlingane, CA, USA), and visualized by 3,3′-diaminobenzidine tetrahydrochloride (DAB) (Zymed Laboratories, South San Francisco, CA, USA). The number of BrdU-positive cells was counted in five fields randomly selected from each section, and three sections at multiple layers for each sample were examined. The BrdU labeling index was calculated as follows: labeling index (%) = (number of cells labeled with BrdU/total cell numbers) × 100.

Apoptosis analysis

Apoptotic cells in tumors were determined by the TUNEL assay using an in situ apoptosis detection kit (Takara Biotechnology, Shiga, Japan). In brief, formalin-fixed sections were processed according to the manufacturer's instruction. The number of apoptotic cells positive for TUNEL staining was counted in five fields randomly selected from each section, and three sections at multiple layers for each sample were examined. The apoptotic index was calculated as follows: apoptotic index (%) = (apoptotic cell number/total cell number) × 100.

Tumor angiogenesis

Immunohistochemical staining of CD34 was used for the analysis of tumor vasculature. Specimens were deparaffinized and incubated with a primary antibody against CD34 (1:500) overnight at 4°C. After rinsing with phosphate-buffered saline (PBS), they were incubated with the biotinylated anti-rat IgG, followed by the ABC method and visualized by DAB. To evaluate tumor vessel formation in each tumor, the area of CD34-positive endothelial cells was quantified by image analysis (Adobe Systems, San Jose, CA, USA).

Statistical analysis

Data are expressed as the mean ± standard error of the mean (SEM). Statistical comparisons between groups were performed with Student's t test. Differences were considered statistically significant at $P < 0.05$.

Results

CD9 is involved in inhibition of tumor growth

We evaluated the antitumor effect of anti-human CD9 mAb ALB6 on the growth of MKN-28 xenografts in SCID mice. The isotype-matched mouse IgG had no significant effect and was used as a negative control in our previous experiment [19, 20]. We measured serum ALB6 concentration after ALB6 was injected intravenously to mice. The serum ALB6 concentration was kept more than 10 μg/body, and its half life was about 8 days (data not shown). We previously examined the specific recognition against CD9 by ALB6 using another anti-CD9 mAb TP82 (Nichirei, Tokyo, Japan). Similarly to ALB, the treatment of MKN-28 cells with TP82 induced apoptosis. Of importance, pretreatment with the TP82 antibody completely blocked the binding of ALB6 to MKN-28 cells. These results suggest that ALB6 really recognizes human CD9 [18]. A representative tumor after the 36th-day treatment is shown in Fig. 1a, where the reduction in tumor size induced by ALB6 treatment can be clearly observed. On the 36th day, the tumor volume of the xenograft in the groups treated with ALB6 was significantly suppressed by approximately 37% compared with that in the control group treated with isotype-matched mouse IgG ($P < 0.05$) (Fig. 1a, b). Thus, these results demonstrated that anti-CD9 antibody ALB6 dramatically reduced the tumorigenicity of MKN-28 xenografts in SCID mice.

Antibody ligation of CD9 inhibits proliferation in gastric cancer cells

At first, we further investigated whether the ALB6-induced inhibition of tumor growth is correlated with cell proliferation of the tumors by immunostaining for BrdU in each group. There were more BrdU-positive cells treated with mouse IgG than those treated with ALB6 (Fig. 2A). The BrdU labeling index in the group treated with ALB6 was significantly decreased by approximately 63% compared with that in the group treated with mouse IgG ($P < 0.01$) (Fig. 2B). Thus, these results demonstrated that anti-CD9 antibody ALB6 dramatically suppressed the cell proliferation of MKN-28 xenografts in SCID mice.

Antibody ligation of CD9 induces apoptosis in gastric cancer cells

We then investigated whether the ALB6-induced inhibition of tumor growth is correlated with cell apoptosis of the tumors. Apoptotic cells in the tumor were determined by TUNEL assay, and apoptotic indexes of the tumors were investigated in each group. TUNEL-positive cells were evident in the cells treated with ALB6, but only a few such cells were observed in cells treated with mouse IgG (Fig. 3A). The apoptotic index in the groups treated with ALB6 was significantly increased by approximately 280% compared with that in the groups treated with mouse IgG ($P < 0.05$) (Fig. 3B). Thus, these results demonstrated that anti-CD9 antibody ALB6 dramatically induced the apoptosis of MKN-28 xenografts in SCID mice.

Antibody ligation of CD9 inhibits angiogenesis in gastric cancer cells

Tumor angiogenesis plays an important role in tumor promotion and progression [22]. Thus, in order to evaluate the effect of ALB6 on tumor angiogenesis, CD34 was immunohistochemically stained and CD34-positive endothelial cells were counted as tumor microvessel density to measure tumor angiogenesis. Tumor microvessel densities in the group treated with ALB6 were significantly suppressed by approximately 60% compared with that in the group treated with mouse IgG ($P < 0.05$) (Fig. 4A, B). Therefore, these results suggest that anti-CD9 antibody ALB6 might inhibit angiogenesis.

Discussion

The incidence and mortality rate of gastric cancer have decreased dramatically over the past several decades [23]. Nonetheless, the disease remains a major public health issue as the fourth most common cancer and the second leading cause of cancer death worldwide [24]. A number of experiments using transfection and Abs specific for CD9 have revealed that this tetraspanin can modify cell motility and migration as well as signals from cell surface receptors [25–29]. Many investigators have suggested that CD9 provides a bridge among cell surface proteins to generate functional complexes, which enhance cell adhesion among tumor cells as well as inhibit tumor cell migration through extracellular layers [4–6]. We have previously reported that the treatment of gastrointestinal cancer cell lines with anti-CD9 Ab induced apoptosis via the selective activation of JNK/SAPK, p38 MAPK, caspase-3, and the p46 Shc isoform, indicating that ALB6 acts as a ligand-like molecule [19]. In addition, many investigators believe that the treatment of cells with ALB6 induces signals for adhesion, migration, and cell survival [7, 25–27], and that ALB6 does not cross-react with the mouse CD9. Based on these observations and literature, we designed an experiment to determine whether CD9 is involved in the tumorigenic process of the development of primary tumors.

In the present study, we have shown the first evidence that anti-CD9 antibody ALB6 inhibited the tumor growth

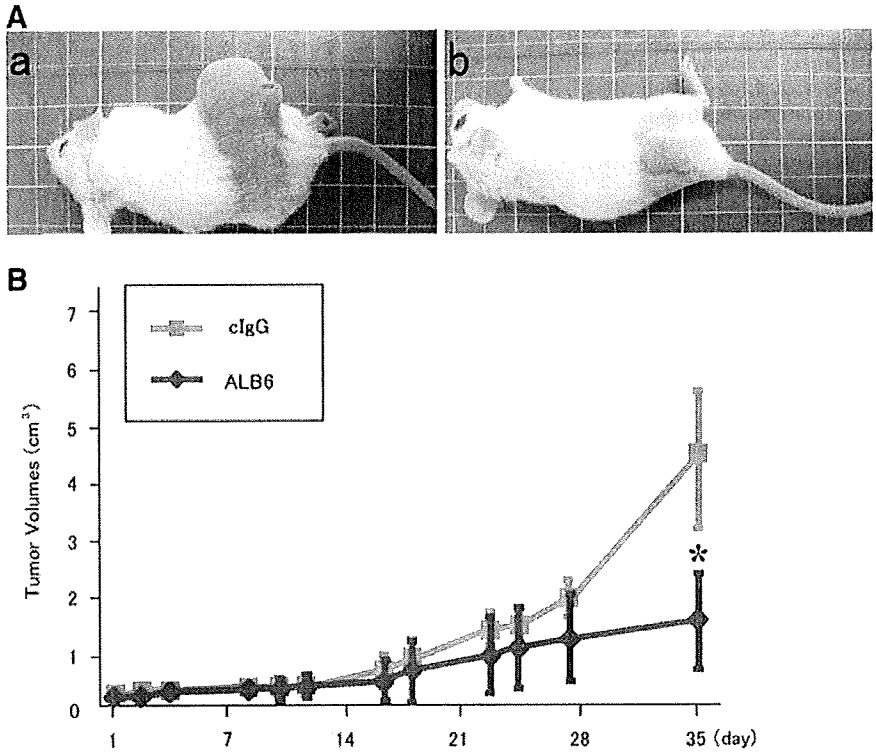

Fig. 1 The antitumor effects of ALB6 on the growth of xenografts in SCID mice. MKN-28 cells were inoculated subcutaneously into the left side of the back of SCID mice (five mice in each group). After visualizing the tumor, 100 μg/body/time ALB6 or isotype-matched mouse IgG was injected intravenously three times at 3-day intervals for the first week (on first, fourth, and seventh day). **A** The photographs show representative tumors of IgG group (**a**) and ALB6 group (**b**) on the 36th day. **B** Tumor volumes (mm^3) expressed as $width^2 \times length \times 0.52$ (mm^3). Data from each treatment group are represented as mean ± SEM of the results in five mice. *Squares* denote control groups, and *diamonds* denote ALB6 groups. $*P < 0.05$ versus control

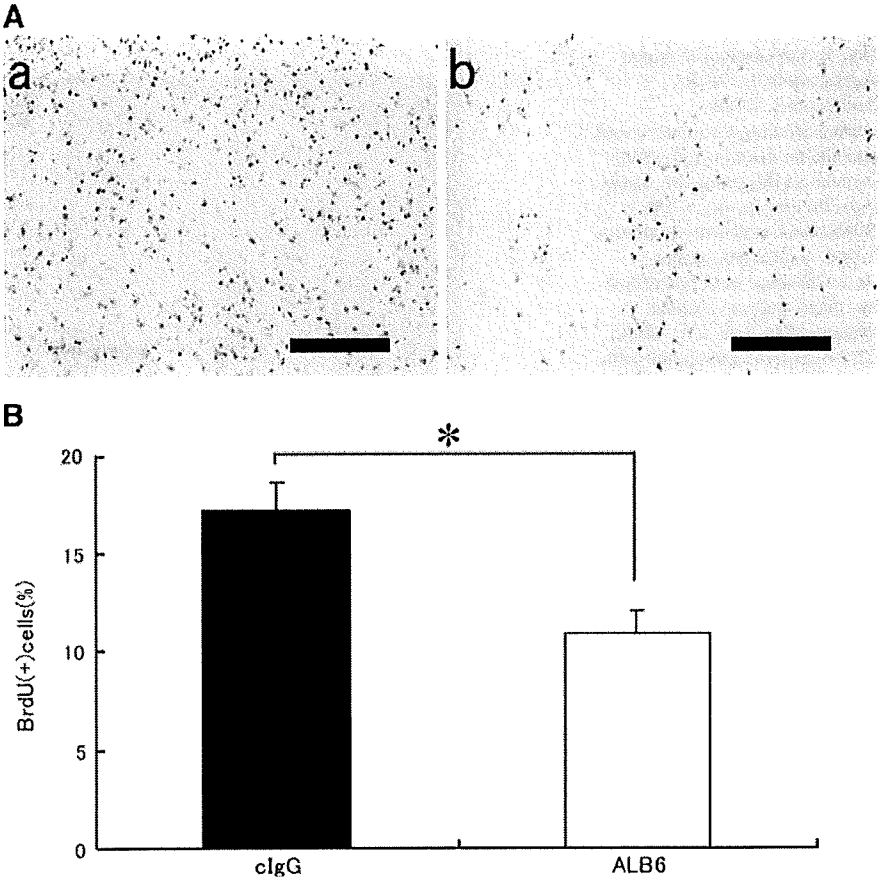

Fig. 2 Inhibition of the cell proliferation in tumors by ALB6 treatment. **A** BrdU-positive cells in tumors in control group (**a**) and ALB6 group (**b**) were visualized as brown staining. *Scale bars* 200 μm (**a**, **b**), ×100. **B** In subcutaneous tumors, the number of proliferating cells was quantified by counting BrdU-positive cells in five different fields randomly selected in three sections at multiple layers for each sample under ×100 magnification. Data from each treatment group are represented as mean ± SEM. $*P < 0.05$ versus control

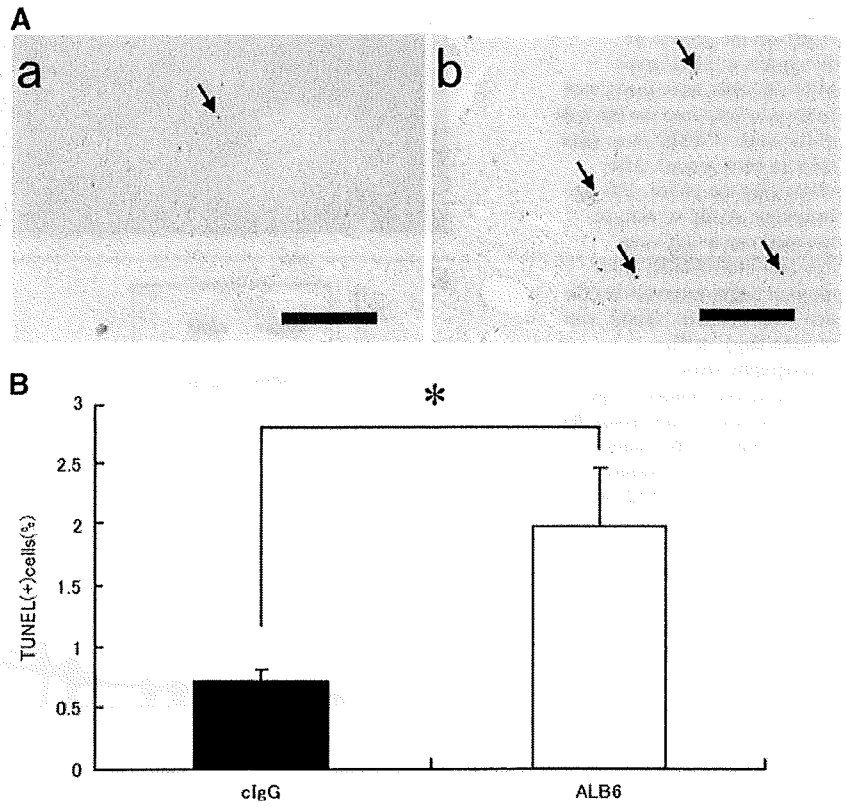

Fig. 3 Induction of apoptosis cells in tumors by ALB6 treatment. **A** Apoptotic cells (*arrow*) in tumors treated with IgG (**a**) or ALB6 (**b**) were visualized as brown staining. *Scale bars* 200 μm (**a**, **b**), ×100. **B** In subcutaneous tumors, apoptotic cells were immunohistochemically detected by the TUNEL method and the number of apoptotic cells was quantified by counting TUNEL-positive cells in five different fields randomly selected in three sections at multiple layers for each sample. Data from each treatment group are represented as mean ± SEM. $*P < 0.05$ versus control

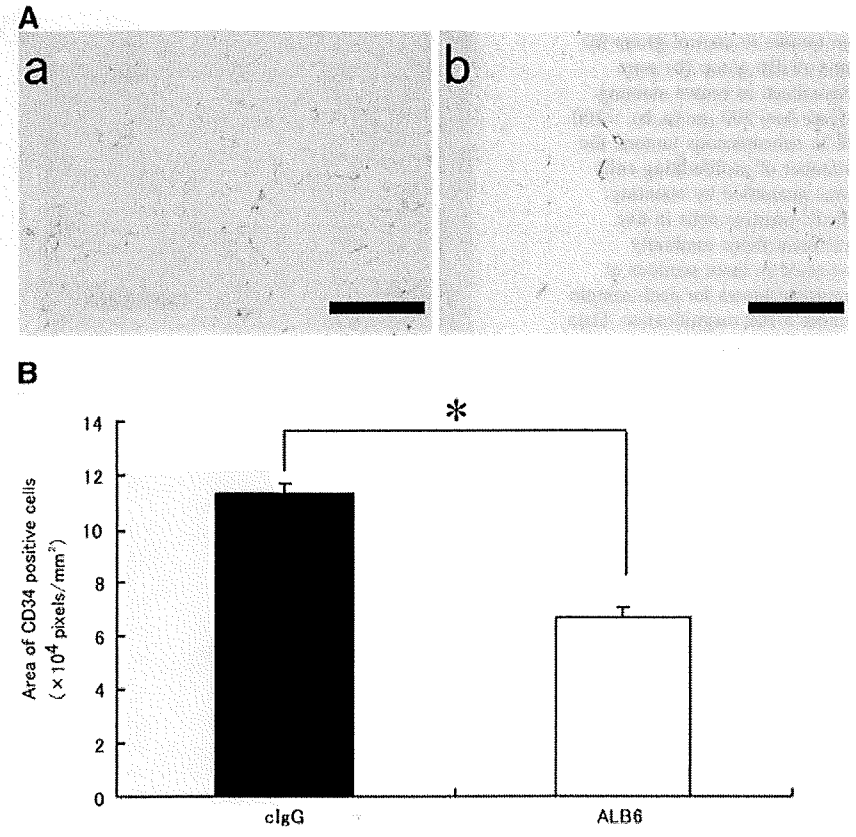

Fig. 4 Suppression of tumor angiogenesis by ALB6 treatment. **A** CD34 immunostaining of tumor vessel endothelial cells in IgG group (**a**) and ALB6 group (**b**). *Scale bars* 200 μm (**a**, **b**), ×100. **B** Microvessel density in tumors in IgG and ALB6 groups. Vascular areas were quantified by image analysis (Adobe Systems, San Jose, CA, USA). CD34-positive endothelial cells in 15 fields in tumors randomly selected under ×100 magnification. Data from each treatment group are represented as mean ± SEM. $*P < 0.05$ versus control

of MKN-28 xenografts in SCID mice. As for the possible functional mechanism, we demonstrated that ALB6 might have therapeutic potential in inducing antiproliferative, apoptotic, and antiangiogenetic effects in gastric cancers. We have previously reported that CD9 associated with EGFR tyrosine kinase caused accelerated ligand-induced clearance of EGFR from the cell surface, resulting in attenuation of EGFR signaling [20]. Thus, this result might help to explain the tumor suppressor activity of CD9. In addition to the antiproliferation effect, in this present study, we have also shown that ALB6 induced some apoptosis in gastric cancer cells. The molecular mechanism of apoptosis induced by ALB6 in gastric cancer cells in vivo needs to be elucidated more clearly in the future.

Tumor growth is dependent on angiogenesis, the formation of new blood vessels [22]. Targeting tumor vessels provides several advantages over traditional antitumor approaches. To further examine the effect of ALB6 on angiogenesis in gastric cancer cells, we estimated tumor microvessel density by counting the number of CD34-positive endothelial cells. Tumor microvessel densities in the ALB6 treatment group were significantly suppressed compared with that in the control IgG treatment group. VEGF-A is a growth factor associated with angiogenesis [30]. Many previous studies have revealed that overexpression of VEGF-A is associated with tumor angiogenesis, nodal metastasis, and a poor prognosis in cancer patients [31]. It has been previously reported that CD9 gene transduction could downregulate VEGF-A expression [32]. Thus, ALB6 might inhibit tumor growth by suppressing angiogenesis by modulating VEGF-A expression. Taken together, in this present study, we have shown a possible beneficial use of CD9 in the treatment of human gastric cancer cells.

Recently, it has been reported that anti-CD9 mAbs inhibited the proliferation of human colon carcinoma cells [33] and ectopic expression of CD9 in small-cell lung carcinoma cells that resulted in inhibition of their proliferation [34], and that adenoviral transduction of CD9 inhibited lymph node metastasis in an orthotopic lung cancer model [35]. These findings strongly suggest that CD9 plays indispensable roles in malignant tumor progression. In addition to its role as a metastasis-suppressor molecule, CD9 might act as a negative regulator of some types of carcinomas.

An abundance of recent evidence suggests that targeting tetraspanins, for example, by monoclonal antibodies, soluble large-loop proteins or RNAi technology, or adenoviral transduction methods, should be therapeutically beneficial [36]. In addition, therapeutic monoclonal antibodies (mAbs) are currently being developed for the treatment of cancer and other diseases. The clinical use of mAb as cancer therapeutics has been realized in the last few years with the approval and successful commercialization of antibody products, such as trastuzumab, rituximab, cetuximab, and bevacizumab [37]. Therefore, CD9 might be an appealing target for antibody therapy for gastric cancer.

We previously reported that CD9 was highly expressed in gastric cancer as compared with the adjacent noncancerous gastric mucosa [17]. In addition, it is reported that CD9 is one of the genes upregulated in gastric cancer by complementary DNA (cDNA) expression microarray [38]. These results suggest that CD9 expression in noncancerous tissues is lower than in gastric cancer tissues. Thus, the side-effects of anti-CD9 antibody treatment on normal gastrointestinal tissues might be tolerable. However, data concerning this issue will be needed in the future.

In this study, we demonstrated that anti-CD9 antibody ALB6 suppressed tumor growth and proliferation, induced apoptosis, and inhibited angiogenesis in human gastric cancer xenografts. These results suggest that CD9 might be a new attractive targeting molecule in gastric cancer therapy.

Acknowledgments This work was supported in part by grants-in-aid (grant 10359846 to S. Tsutsui) from the Ministry of Education, Science, Sports, and Culture of Japan.

References

1. WHO. World Health Organization fact sheet no. 297: cancer WHO fact sheet, vol 2007. WHO, 2006.
2. Jemal A, Siegel R, Ward E, Murray T, Xu J, Smigal C, et al. Cancer statistics. CA Cancer J Clin. 2006;56:106–30.
3. Gallo A, Cha C. Updates on esophageal and gastric cancers. World J Gastroenterol. 2006;12:3237–42.
4. Maecker HT, Todd SC, Levy S. The tetraspanin superfamily: molecular facilitators. FASEB J. 1997;1:428–42.
5. Berditchevski F. Complexes of tetraspanins with integrins: more than meets the eye. J Cell Sci. 2001;14:4143–51.
6. Hemler ME. Tetraspanin proteins mediate cellular penetration, invasion, and fusion events and define a novel type of membrane microdomain. Ann Rev Cell Dev Biol. 2003;19:397–422.
7. Boucheix C, Rubinstein E. Tetraspanins. Cell Mol Life Sci. 2001;58:1189–205.
8. Hemler ME. Tetraspanin functions and associated microdomains. Nat Rev Mol Cell Biol. 2005;10:801–11.
9. Miyake M, Koyama M, Seno M, Ikeyama S. Identification of the motility-related protein (MRP-1), recognized by monoclonal antibody M31–15, which inhibits cell motility. J Exp Med. 1991;174:1347–54.
10. Higashiyama M, Taki T, Ieki Y, Adachi M, Huang CL, Koh T, et al. Reduced motility related protein-1 (MRP-1/CD9) gene expression as a factor of poor prognosis in non-small cell lung cancer. Cancer Res. 1995;55:6040–4.
11. Huang CI, Kohno N, Ogawa E, Adachi M, Taki T, Miyake M. Correlation of reduction in MRP-1/CD9 and KAI1/CD82 expression with recurrences in breast cancer patients. Am J Pathol. 1998;153:973–83.
12. Mori M, Mimori K, Shiraishi T, Haraguchi M, Ueo H, Barnard GF, et al. Motility related protein 1 (MRP1/CD9) expression in colon cancer. Clin Cancer Res. 1998;4:1507–10.

13. Sho M, Adachi M, Taki T, Hashida H, Konishi T, Huang CL, et al. Transmembrane 4 superfamily as a prognostic factor in pancreatic cancer. Int J Cancer. 1998;79:509–16.
14. Houle CD, Ding XY, Foley JF, Afshari CA, Barrett JC, Davis BJ. Loss of expression and altered localization of KAI1 and CD9 protein are associated with epithelial ovarian cancer progression. Gynecol Oncol. 2002;86:69–78.
15. Cajot JF, Sordat I, Silvestre T, Sordat B. Differential display cloning identifies motility-related protein (MRP1/CD9) as highly expressed in primary compared to metastatic human colon carcinoma cells. Cancer Res. 1997;57:2593–7.
16. Uchida S, Shimada Y, Watanabe G, LiZ Gang, Hong T, Miyake M, et al. Motility-related protein (MRP-1/CD9) and KAI1/CD82 expression inversely correlate with lymph node metastasis in oesophageal squamous cell carcinoma. Br J Cancer. 1999;79: 1168–73.
17. Murayama Y, Miyagawa J, Shinomura Y, Kanayama S, Isozaki K, Yamamori K, et al. Significance of the association between heparin-binding epidermal growth factor-like growth factor and CD9 in human gastric cancer. Int J Cancer. 2002;98:505–13.
18. Hori H, Yano S, Koufuji K, Takeda J, Shirouzu K. CD9 expression in gastric cancer and its significance. J Surg Res. 2004;117:208–15.
19. Murayama Y, Miyagawa J, Oritani K, Yoshida H, Yamamoto K, Kishida O, et al. CD9-mediated activation of the p46 Shc isoform leads to apoptosis in cancer cells. J Cell Sci. 2004;117:3379–88.
20. Murayama Y, Shinomura Y, Oritani K, Miyagawa J, Yoshida H, Nishida M, et al. The tetraspanin CD9 modulates epidermal growth factor receptor signaling in cancer cells. J Cell Physiol. 2008;216:135–43.
21. Kuba K, Matsumoto K, Date K, Shimura H, Tanaka M, Nakamura T. HGF/NH4, a four-kringle antagonist of hepatocyte growth factor, is an angiogenesis inhibitor that suppresses tumor growth and metastasis in mice. Cancer Res. 2000;60:6737–43.
22. Folkman J. Anti-angiogenesis: new concept for the therapy of solid tumors. Ann Surg. 1972;175:409–16.
23. Desai AM, Pareek M, Nightingale PG, Fielding JW. Improving outcomes in gastric cancer over 20 years. Gastric Cancer. 2004;7:196–203.
24. Crew KD. Epidermiology of gastric cancer. World J Surg. 2006;12:354–62.
25. Jones PH, Bishop LA, Watt FM. Functional significance of CD9 association with beta 1 integrins in human epidermal keratinocytes. Cell Adhes Commun. 1996;4:297–305.
26. Inui S, Higashiyama S, Hashimoto K, Higashiyama M, Yoshikawa K, Taniguchi N. Possible role of coexpression of CD9 with membrane-anchored heparin-binding EGF-like growth factor and amphiregulin in cultured human keratinocyte growth. J Cell Physiol. 1997;171:291–8.
27. Baudoux B, Castanares-Zapatero D, Leclercq-Smekens M, Berna N, Poumay Y. The tetraspanin CD9 associates with the integrin alpha6beta4 in cultured human epidermal keratinocytes and is involved in cell motility. Eur J Cell Biol. 2000;79:41–51.
28. Ikeyama S, Koyama M, Yamaoko M, Sasada R, Miyake M. Suppression of cell motility and metastasis by transfection with human motility-related protein (MRP-1/CD9) DNA. J Exp Med. 1993;177:1231–7.
29. Miyado K, Yamada G, Yamada S, Hasuwa H, Nakamura Y, Ryu F, et al. Requirement of CD9 on the egg plasma membrane for fertilization. Science. 2000;287:321–4.
30. Dvorak HF, Brown LF, Detmar M, Dvorak AM. Vascular permeability factor/vascular endothelial growth factor, microvascular hyperpermeability, and angiogenesis. Am J Pathol. 1995; 146:1029–39.
31. Masuya D, Huang C, Liu D, Kameyama K, Hayashi E, Yamauchi A, et al. Introtumoral expression of vascular endothelial growth factor and interleukin-8 associated with angiogenesis in nonsmall cell lung carcinoma patients. Cancer. 2001;92:2628–38.
32. Huang C, Liu D, Masuya D, Kameyama K, Takashi Nakashima T. MRP-1/CD9 gene transduction downregulates Wnt signal pathways. Oncogene. 2004;23:7475–83.
33. Ovalle S, Gutierrez-Lopez MD, Olmo N, Turnay J, Lizarbe MA, Majano P, et al. The tetraspanin CD9 inhibits the proliferation and tumorigenicity of human colon carcinoma cells. Int J Cancer. 2007;121:2140–52.
34. Zheng R, Yano S, Zhang H, Nakataki E, Tachibana I, Kawase I, et al. CD9 overexpression suppressed the liver metastasis and malignant ascites via inhibition of proliferation and motility of small-cell lung cancer cells in NK cell-depleted SCID mice. Oncol Res. 2005;15:365–72.
35. Takeda T, Hattori N, Tokuhara T, Nishimura Y, Yokoyama M, Miyake M. Adenoviral transduction of MRP-1/CD9 and KAI1/CD82 inhibits lymph node metastasis in orthotopic lung cancer model. Cancer Res. 2007;67:1744–9.
36. Hemler ME. Targeting of tetraspanin proteins–potential benefits and strategies. Nat Rev Drug Discov. 2008;7:747–58.
37. Bernard J, Scallon LA, Snyder G, Mark A, Qiming C, Li Y, et al. A review of antibody therapeutics and antibody-related technologies for oncology. J Immunother. 2006;29:351–64.
38. Liu LX, Liu ZH, Jiang HC, Qu X, Zhang WH, Wu LF, et al. Profiling of differentially expressed genes in human gastric carcinoma by cDNA expression array. World J Gastroenterol. 2002;8:580–5.

GASTROENTEROLOGY 2009;137:188–198

Deficiency of GMDS Leads to Escape from NK Cell-Mediated Tumor Surveillance Through Modulation of TRAIL Signaling

KENTA MORIWAKI,* KATSUHISA NODA,*,‡ YOICHI FURUKAWA,§ KENJI OHSHIMA,‖ AIRI UCHIYAMA,‖ TSUTOMU NAKAGAWA,* NAOYUKI TANIGUCHI,‖,¶ YATARO DAIGO,# YUSUKE NAKAMURA,# NORIO HAYASHI,‡ and EIJI MIYOSHI*,‖

*Departments of *Molecular Biochemistry and Clinical Investigation, ‡Gastroenterology and Hepatology, and ‖Biochemistry, Osaka University Graduate School of Medicine, Osaka, Japan; §Division of Clinical Genome Research and #Laboratory of Molecular Medicine, Human Genome Center, Institute of Medical Science, The University of Tokyo, Tokyo, Japan; and ¶Department of Disease Glycomics, Research Institute for Microbial Diseases, Osaka University, Center for Advanced Science and Innovation, Osaka, Japan*

See editorial on page 36.

BACKGROUND & AIMS: Tumor necrosis factor-related apoptosis-inducing ligand (TRAIL) promotes apoptosis in cancer cells, but not normal cells, and is critically involved in tumor rejection through natural killer (NK) cell–mediated immune surveillance. Oligosaccharides are involved in various aspects in carcinogenesis, and fucosylation is one of the most important oligosaccharide modifications in cancer. Here, we report for the first time mutations of the GDP-mannose-4,6-dehydratase (*GMDS*) gene, which plays a pivotal role in fucosylation, in human colon cancer. The mutations resulted in resistance to TRAIL-induced apoptosis followed by escape from immune surveillance. **METHODS:** The mock and *GMDS*-rescued HCT116 cells were investigated in terms of NK cell–mediated tumor surveillance by TRAIL signaling both in vitro and in vivo. The mutational analysis for *GMDS* was performed with kinds of cancer cell lines and tissues. **RESULTS:** The mutation found here led to a virtually complete deficiency of cellular fucosylation, and transfection of the wild-type *GMDS* into HCT116 cells restored the cellular fucosylation. When mock and *GMDS*-rescued cells were transplanted into athymic mice, tumor growth and metastasis of the *GMDS*-rescued cells were dramatically suppressed through NK cell–mediated tumor surveillance. Furthermore, the *GMDS*-rescued cells showed high susceptibility to TRAIL-induced apoptosis, and anti-TRAIL blocking antibody suppressed the accelerated direct cell lysis of the *GMDS*-rescued cells by splenocytes. Similar mutations of the *GMDS* were found in certain human cancer tissues and other cell lines. **CONCLUSIONS: This pathway by *GMDS* mutation could be a novel type of cancer progression through cellular fucosylation and NK cell–mediated tumor surveillance.**

Glycosylation has been found to be involved in tumor malignancy, developmental processes, and the immune system, which has led to new insights into many human diseases.[1–3] In cases of colon cancer, many reports have suggested that changes in glycosylation are involved in the carcinogenesis and metastasis.[4,5] The prognosis of colorectal cancer in stage I or II has been reported relatively good, and 5-year survival rates are approximately 90% or 80%, respectively.[6] However, certain cases of colorectal cancer develop distant metastasis or peritoneal dissemination rapidly, which would depend on the abnormality of apoptosis signaling, the resistance to immune system, and unknown mechanisms.[7,8] Oligosaccharides are involved in various aspects in carcinogenesis, and fucosylation is one of the most important oligosaccharide modifications in cancer and inflammation.[9–12] Fucosylation is catalyzed by several kinds of fucosyltransferases, which require guanosine diphosphate (GDP)-fucose as a donor substrate. Most GDP-fucose is synthesized by the de novo pathway, in which GDP-mannose is transformed into GDP-fucose through 3 steps that are catalyzed by GDP-mannose-4,6-dehydratase (*GMDS*)[13,14] and GDP-4-keto-6-deoxymannose-3,5-epimerase-4-reductase (FX)[15] (Figure 1). FX knockout mice showed an embryonic lethality phenotype because of a virtually complete deficiency of cellular global fucosylation.[16] This phenomenon enabled us to conclude that fucosylated oligosaccharides are involved in early growth and development as well as many pathologic conditions, especially cancer and inflammation. Recently, it was reported that up-regulation of fucosylation was observed at the early stage of colon calcinogenesis.[17]

Tumor necrosis factor-related apoptosis-inducing ligand (TRAIL) is a type II transmembrane protein that belongs to the tumor necrosis factor superfamily.[18]

Abbreviations used in this paper: AAL, *Aleuria aurantia* lectin; bp, base pair; CMA, concanamycin A; FX, GDP-4-keto-6-deoxymannose-3,5-epimerase-4-reductase; GDP, guanosine diphosphate; *GMDS*, GDP-mannose-4,6-dehydratase; IgG, immunoglobulin G; NK, natural killer; PARP, poly(ADP-ribose) polymerase; RT-PCR, reverse transcription–polymerase chain reaction; siRNA, small interfering RNA; TRAIL, tumor necrosis factor-related apoptosis-inducing ligand; WT, wild-type.

0016-5085/09/$36.00
doi:10.1053/j.gastro.2009.04.002

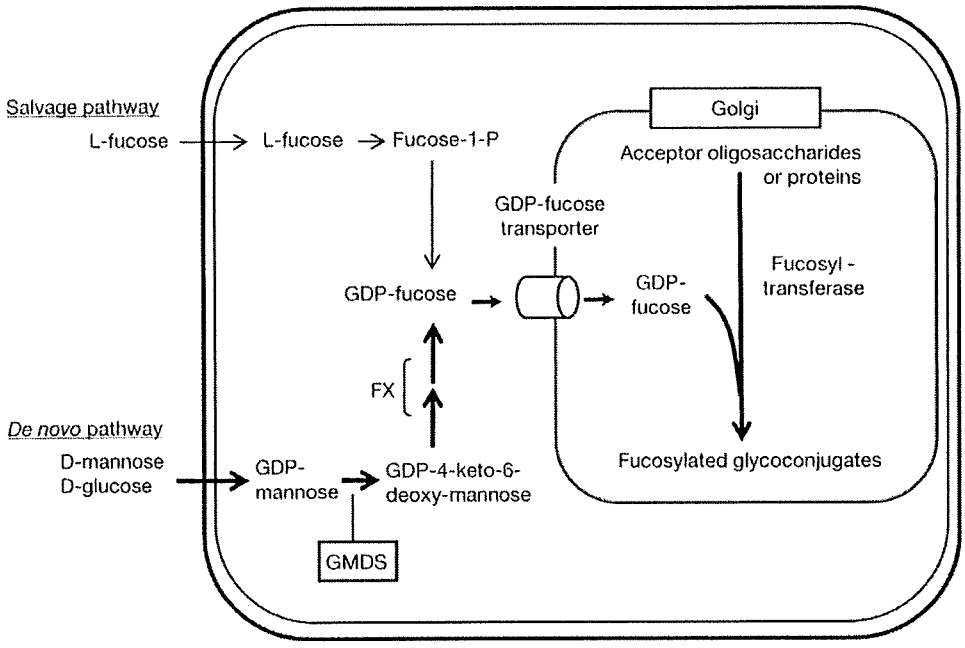

Figure 1. Fucose metabolism. GDP-fucose is mainly synthesized through the de novo pathway by 3 reactions catalyzed by *GMDS* and FX. Free L-fucose is converted to GDP-fucose through the salvage pathway, which is a minor pathway. GDP-fucose is subsequently transported from the cytosol to the Golgi lumen by GDP-fucose transporter, and then transferred to acceptor oligosaccharides and proteins by fucosyltransferases.

TRAIL can initiate apoptosis in a wide variety of tumor cells, but not normal cells, through interaction with TRAIL receptors. The engagement of TRAIL receptors by the ligand leads to the recruitment of a cytoplasmic adaptor protein, such as Fas-associated death domain, which in turn activates caspase-8 and -10. Caspase-8 either directly activates downstream effector caspase-3, -6, and -7, or the intrinsic pathway through Bid cleavage, leading to apoptosis.[19,20] TRAIL-deficient mice were more sensitive to experimental and spontaneous tumor metastasis and to chemical carcinogenesis.[21] The administration of anti-TRAIL functional blocking antibody significantly increased experimental liver metastases of TRAIL-sensitive tumor cells through inhibition of natural killer (NK) cell–mediated tumor surveillance.[22] TRAIL receptor–deficient mice also showed high sensitivity to tumorigenesis, chronic inflammation,[23] and tumor metastasis.[24] These reports substantiate that TRAIL is an important natural effector molecule against transformed cells in host defense. From the aspect of a clinical approach, optimized soluble recombinant human TRAIL or agonistic antibodies targeting TRAIL receptors are promising proapoptotic antitumor therapeutic agents currently undergoing phase 1or 2 clinical evaluation in patients with several types of tumors.[25] However, it has now become clear that many types of tumor cells are resistant to TRAIL.[26–28] Thus, it is critical to clarify the biologic determinants of susceptibility to TRAIL-mediated apoptosis.

In the present study, we found a virtually complete deficiency of fucosylation resulting from an alteration of *GMDS* transcripts in a human colon cancer cell line, HCT116, which resulted in escape from the immune surveillance system because of resistance to TRAIL-induced cell death. This alteration of *GMDS* would be a novel trigger of the progression of colon cancer by escape from TRAIL-mediated cell death.

Materials and Methods

Cell Lines and Materials

Human colon cancer cell lines, DLD-1, WiDr, and HCT116, were provided by the American Type Culture Collection (Manassas, VA), and NCI-H716 and LS174T cells were kindly provided by Dr Y. Nakamura. SCH cells were provided by the Human Science Research Resources Bank (Osaka, Japan). SCH cells, synthesize human chorionic gonadotropin, were established by Kameya et al[29] from a metastatic omental lesion of gastric choriocarcinoma derived from a 46-year-old man. These cells were cultured in RPMI1640 supplemented with 100 U/mL penicillin, 100 μg/mL streptomycin, and 10% fetal calf serum. Both human and mouse recombinant TRAIL were obtained from BIOMOL (Plymouth Meeting, PA). All colorectal cancer tissues and corresponding noncancerous tissues were obtained with informed consent from surgical specimens of patients who underwent surgery.

Lectin Blot and Western Blot Analysis

Lectin blot and Western blot analysis was performed as described previously.[30] Rabbit anti-*GMDS* antibody was established as described previously.[30] Rabbit anti-cleaved poly(ADP-ribose) polymerase (PARP), β-actin, and horseradish peroxidase–conjugated anti-rabbit immunoglobulin G (IgG) antibody as a second antibody were purchased from Cell Signaling (Beverly, MA).

Measurement of the Cytosolic GDP-Fucose Concentration

Measurement of the cytosolic GDP-fucose concentration was performed as described previously.[31]

Transfection of the Wild-Type and Mutant GMDS

pcDNA3.1/Hyg (Invitrogen, Carlsbad, CA) vector carrying human wild-type (WT) *GMDS* was transfected into HCT116 cells with the FuGENE 6 transfection reagent (Roche, Basel, Switzerland) according to the manufacturer's protocol. Selection was performed by the addition of Hygromycin B (Calbiochem, Darmstadt, Germany) at 150 μg/mL. Each mutation was introduced by polymerase chain reaction (PCR) amplification with the use of PrimeSTAR HS DNA polymerase (TAKARA BIO, Shiga, Japan) and an above vector as template. The PCR primers are summarized in Supplementary Table 1. All mutations were verified by DNA sequencing.

Cell Growth Assay

Cells were seeded onto 96-well plates at 2500 cells/well and then cultured. After the addition of a WST-8 solution (Dojindo Laboratory, Kumamoto, Japan), the cells were reacted for 3 hours. WST is a highly water-soluble disulfonated tetrazolium salt. Then the absorbance of the formazan product formed was detected at 450 nm. The results are represented as the means of 3 experiments.

Animal Experiments

Cells (6.0×10^6) were subcutaneously injected into 5-week-old female BALB/c nu/nu athymic nude mice (Japan SLC Inc, Shizuoka, Japan). Tumor weight and size were determined. In some experiments, mice were administered 200 μg of anti-asialo GM1 antibody (Wako, Osaka, Japan) or control rat IgG (Sigma, St Louis, MO) at 1 day before and 1, 6, and 11 days after tumor inoculation for the depletion of NK cells. For experimental metastasis, 1.0×10^6 cells were injected into the spleens of 5-week-old female BALB/c nu/nu athymic nude mice. At 4 weeks after injection, the mice were killed under anesthesia. Tumor formation in the liver and peritoneum was evaluated and also histologically examined after H&E staining. These mice were maintained under specific pathogen-free conditions in the Institute of Experimental Animal Sciences, Osaka University Medical School. All of these animal experiments were approved by the ethical committee of Osaka University Graduate School of Medicine.

FACS Analysis

To determine the sub-G_1 DNA content, both adherent and floating cells were collected and washed twice with phosphate-buffered saline, and then fixed in ice-cold 50% ethanol. After the addition of RNase, the cells were stained with propidium iodide (Sigma). The cells were sorted according to their DNA content with FACSCalibur and analyzed with Modifit software (Becton Dickinson, San Diego, CA). Cell debris and fixation artifacts were gated out. The cells containing subG_1 DNA were calculated as a percentage of the total cells. The results are represented as the means of 3 experiments.

Cytotoxicity Assay

A standard ^{51}Cr release assay was performed. ^{51}Cr-labeled target cells and effector cells were mixed in the U-bottom wells of a 96-well microtiter plate at the indicated E:T ratios. After 8 hours of incubation, cell-free supernatants were collected, and radioactivity was measured with a gamma counter. The results are represented as the means of 3 experiments. In some experiments, the effector cells were pretreated with 50 nmol/L concanamycin A (CMA; Sigma), 10 μg/mL anti-mouse Fas ligand antibody (MFL3; eBioscience, San Diego, CA), or 10 μg/mL anti-mouse TRAIL antibody (N2B2; Becton Dickinson) for 2 hours. Armenian hamster and rat IgG were used as isotype-matched controls for anti-Fas ligand and TRAIL antibody, respectively.

Clonogenic Survival Assay

Tumor cells were plated in 6-well plate at 1200 cells/well. After overnight attachment, cells were treated with various concentrations of TRAIL (BIOMOL) for 2 days. The medium was subsequently changed every 2 days, and the resulting colonies were stained with crystal violet and photographed after 10 days.

Results

Identification of Aberrant Transcripts of GMDS *in HCT116 Cells That Exhibit a Deficiency of Cellular Fucosylation*

When we performed Western blotting with *Aleuria aurantia* lectin (AAL), which binds to fucosylated oligosaccharides,[32] to examine the fucosylation levels in several colon cancer cell lines, a marked decrease in the fucosylation level was found in HCT116 cells (Figure 2*A*). The level of cellular fucosylation depends more on the GDP-fucose level than the activity of fucosyltransferases.[9] When GDP-fucose in these cell lines was assayed by the method we reported previously,[31] it was found to be at an undetectable level in HCT116 cells. A sensitivity limit for GDP-fucose in this assay is <15 pmol/mg. The levels of GDP-fucose in DLD-1 and WiDr cells were 419.2 and 390.8 pmol/mg, respectively. Both *GMDS* and FX are rate-limiting enzymes for the synthesis of GDP-fucose (Figure 1). Reverse transcription (RT)-PCR analyses of both genes showed that the *GMDS* mRNA in HCT116 cells was shorter by approximately 400 base pairs (bp) than that of the wild-type *GMDS* in other colon cancer cells (Figure 2*B*). The sizes and amounts of FX mRNA in all cells examined were almost the same. Sequence analysis showed a deletion of 426 bp in the cDNA of HCT116

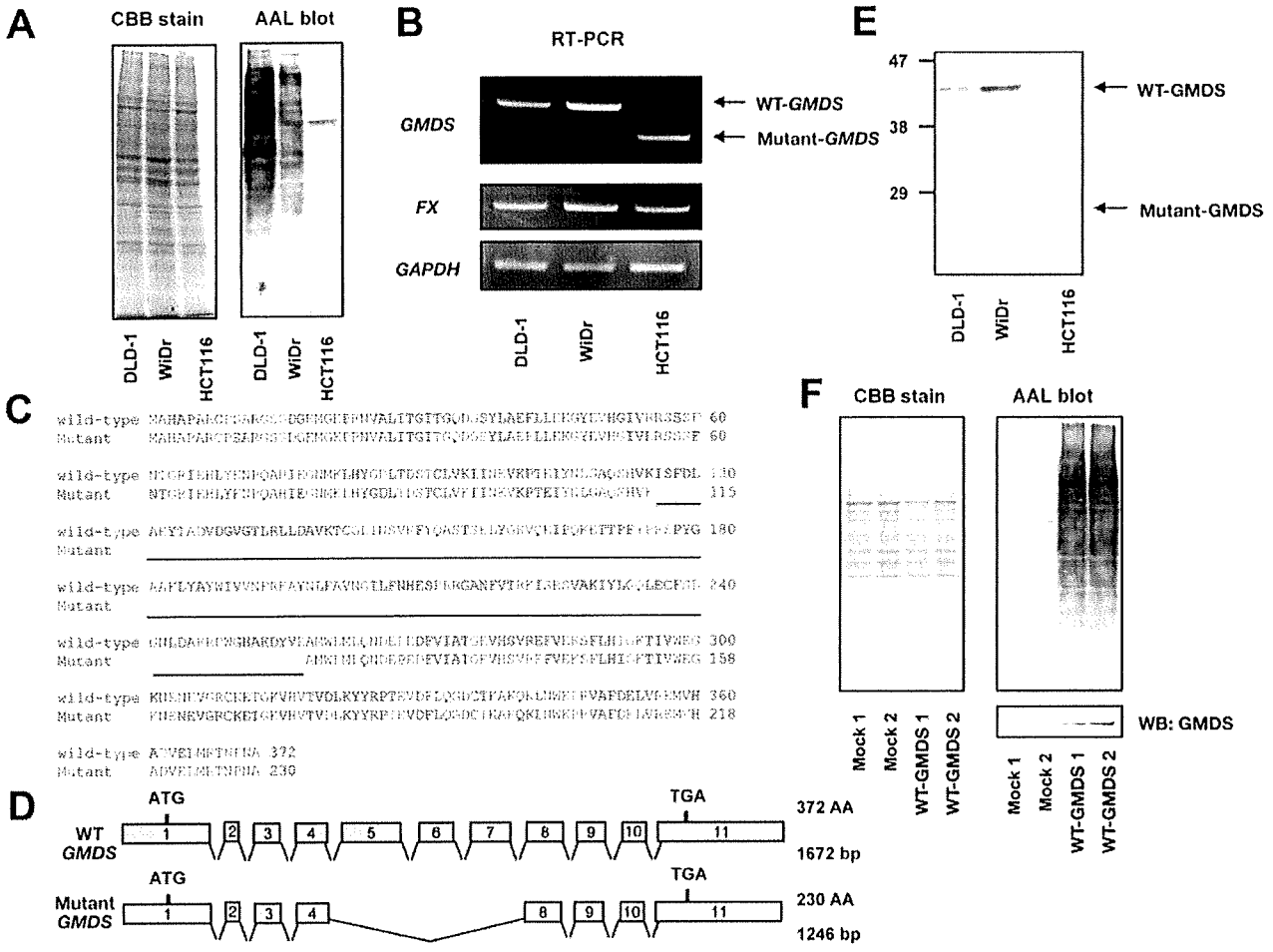

Figure 2. Identification of spontaneous aberrant transcripts of *GMDS* in HCT116 cells. (*A*) The expression patterns of fucosylated glycoproteins in 3 colon cancer cell lines, DLD-1, WiDr, and HCT116, were investigated by AAL blot analysis. Coomassie brilliant blue (CBB) staining indicated that equal amounts of protein were loaded in each lane. (*B*) The expression patterns of GMD and FX mRNA in DLD-1, WiDr, and HCT116 cells were investigated by RT-PCR analysis. The primers used in this experiment were summarized in Supplementary Table 1. Alignment of the protein sequences (*C*) and genomic organization (*D*) of the WT *GMDS* and mutant *GMDS* in HCT116 cells. (*E*) Western blotting with anti-*GMDS* antibody was performed in DLD-1, WiDr, and HCT116 cells. The truncated *GMDS* protein was not detected in HCT116 cells. (*F*) After transfection of an expression vector for WT *GMDS* into HCT116 cells, Western blot analysis of *GMDS* and AAL blot analysis were performed. The expression of the WT *GMDS* protein and strong binding to AAL were observed in 2 transfected cells (WT-*GMDS* 1 and 2).

cells, which corresponds to exons 5, 6, and 7 encoding functionally critical domains for *GMDS* enzyme activity (Figure 2*C* and *D*). This deletion does not cause a frameshift or the appearance of a premature stop codon. Although this aberrant *GMDS* transcript should produce a shorter form of mutant protein, we could not detect the mutant *GMDS* protein of the corresponding molecular weight in HCT116 cells on Western blot analysis (Figure 2*E*). The *GMDS* protein translated from the aberrant transcripts might be very unstable and rapidly degraded because of misfolding with a deletion of 142 amino acids. Transfection of the WT *GMDS* into HCT116 cells restored cellular fucosylation, which was confirmed on AAL blotting (Figure 2*F*). These results indicate that HCT116 cells express abnormal *GMDS* mRNA, leading to inactivation of the de novo pathway for GDP-fucose synthesis followed by a deficiency of cellular fucosylation.

Suppression of Tumor Growth and Metastasis In Vivo on the Restoration of Fucosylation

To investigate the tumor growth of fucosylation-negative (mock cells) or -positive (*GMDS*-rescued cells) colon cancer cells in vivo, we subcutaneously injected mock and *GMDS*-rescued cells into athymic mice. We found that the tumor growth was dramatically decreased in the *GMDS*-rescued cells compared with the mock cells (Figure 3*A*). Furthermore, we evaluated the effect of fucosylation on tumor metastasis. When these cells were injected into the spleens of athymic mice, the metastatic tumor formation in the liver and peritoneum was also

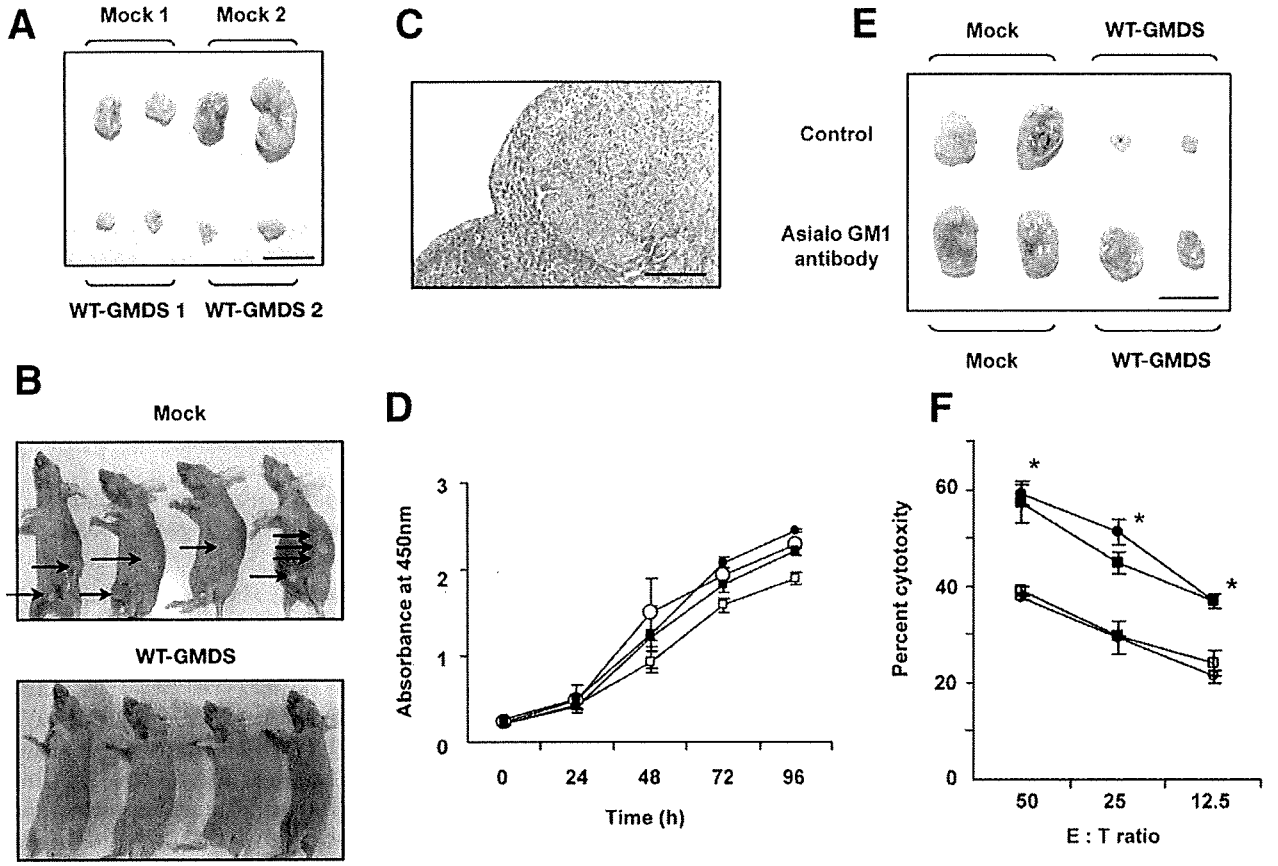

Figure 3. Contribution of NK cells to suppression of tumor growth on the complementation of WT *GMDS*. (*A*) Tumors grown on the backs of athymic mice were excised at 20 days after subcutaneous injection and photographed. The *bar* indicates 10 mm. (*B*) At 4 weeks after injecting tumor cells into the spleens of athymic mice, the mice were killed and photographed. *Arrowheads* indicate large peritoneal metastases. The results of these experiments are given in Table 1. (*C*) Tumor formation in the liver was histologically examined after H&E staining. The bar indicates 200 μm. (*D*) The in vitro growth rate was investigated by WST assay. *Bars* indicate SD. (*E*) Athymic mice were treated with either anti-asialo GM1 or control rabbit IgG. Mice were killed at 17 days to examine tumor growth in vivo. The bar indicates 10 mm. (*F*) The sensitivities of tumor cells to the direct cytotoxicity of splenocytes from athymic mice were investigated by ^{51}Cr-releasing assay. E indicates effecter cells (splenocytes); T, target cells (tumor cells); *open circles*, mock 1; *open squares*, mock 2; *filled circles*, WT-*GMDS* 1; and *filled squares*, WT-*GMDS* 2. *Asterisks* indicate significant difference between mock and WT-*GMDS* cells ($P < .05$, unpaired I test). *Bars* indicate SD.

decreased in the case of the *GMDS*-rescued cells (Figure 3*B*). Histologic examination of tumors in the livers from the mice injected with the mock cells showed liver metastasis (Figure 3*C*). The results of in vivo experiments are summarized in Table 1. In contrast, the cell growth rate in vitro did not differ between mock and *GMDS*-rescued cells (Figure 3*D*). These results indicate that the deficiency of fucosylated oligosaccharides resulted in the acceleration of tumor growth and metastasis in vivo, which was independent of the cell growth rate.

Table 1. The Suppression of Subcutaneous or Metastatic Tumor Formation by the *GMDS*-Rescued Cells in Athymic Mice

	Subcutaneous tumor formation[a]			Metastatic tumor formation		
Cells	Tumor weight (*g*)	Major axis (*mm*)	Minor axis (*mm*)	Liver tumor	Peritoneum tumor	Body weight (*g*) (n = 8)
Mock	0.23 ± 0.13	9.19 ± 4.00	5.29 ± 2.24	12/16	15/16	15.66 ± 1.62
WT-*GMDS*	0.06 ± 0.02[b]	4.00 ± 1.41[b]	2.03 ± 0.50[b]	1/16[c]	3/16[c]	18.60 ± 1.83[c]

[a]The results are presented as mean values ± SDs (n = 9).
[b]$P < .01$, compared with mock cells with an unpaired *t* test.
[c]$P < .01$, compared with mock cells with Fisher's test.

NK Cells Critically Contribute to the Suppression of Tumor Growth Through the Restoration of Fucosylation

Balb/c athymic mice are defective in T-cell–dependent immune responses. Therefore, NK cells play a critical role in the rejection of implanted cancer cells by the immune surveillance system in the mice. To determine whether NK cells are involved in the suppression of tumor growth of the *GMDS*-rescued cells, NK cells were depleted by injecting anti-asialo GM1 antibody. The rate of depletion of NK cells was approximately 85% in anti-asialo GM1 antibody-injected athymic mice compared with control IgG-injected mice, which was confirmed by investigation of DX5-positive cells with flow cytometry (data not shown). As shown in Figure 3*E*, depletion of NK cells stimulated tumor growth of the *GMDS*-rescued cells that had been subcutaneously injected. Subsequently, to determine the sensitivity to cell lysis by splenocytes from athymic mice, splenocytes were isolated from athymic mice, followed by stimulation with mouse interleukin-2 for 48 hours, and then the cytotoxicity assay was performed for mock and *GMDS*-rescued cells. As shown in Figure 3*F*, the *GMDS*-rescued cells showed higher sensitivity to cell lysis by the isolated splenocytes compared with the mock cells. These results indicate that NK cells critically contribute to the suppression of tumor growth of the *GMDS*-rescued cells. Therefore, the deficiency of fucosylation in HCT116 cells leads to escape from NK cell–mediated immune surveillance.

Increased Tumor Rejection in GMDS-*Rescued Cells Because of NK Cell–Mediated Immune Surveillance Depends on Increased Susceptibility to TRAIL*

NK cells exert their lytic function through the perforin-granzyme, Fas ligand, and TRAIL pathways. Fas ligand and TRAIL induce tumor apoptosis through the corresponding transmembrane death receptors, which are modified by oligosaccharides. It is possible that changes in the fucosylation of these death receptors affect their signaling. The susceptibility to TRAIL was investigated for mock and *GMDS*-rescued cells. Clonogenic survival on treatment with TRAIL was dramatically decreased for the *GMDS*-rescued cells compared with the mock cells (Figure 4*A*). A significant increase in the sub-G_1 population, which is a hallmark of apoptosis, of the *GMDS*-rescued cells after the treatment with TRAIL was also observed (Figure 4*B*). Western blotting of cleaved PARP, which serves as a marker of cells undergoing apoptosis, showed a higher level of apoptosis in the *GMDS*-rescued cells, in a dose-dependent manner, on human or mouse TRAIL treatment (Figure 4C). Murine TRAIL is active toward human cells, as reported previously.[18] These results indicated that the *GMDS*-rescued cells showed higher susceptibility to TRAIL than the mock cells and that a deficiency of fucosylation in cancer cells resulted in resistance to TRAIL-mediated apoptosis. To determine whether the increased susceptibility to TRAIL of the *GMDS*-rescued cells was involved in the increase in tumor rejection by NK cells, anti-TRAIL blocking antibody was used in a cytotoxicity assay. As shown in Figure 4*D*, cell lysis of the *GMDS*-rescued cells by splenocytes was markedly suppressed in the presence of anti-TRAIL blocking antibody. In contrast, treatment with anti-Fas blocking antibody or CMA, which inhibits perforin-mediated killing, did not affect the difference in cell lysis by splenocytes between mock and *GMDS*-rescued cells. These results indicate that the increased susceptibility to TRAIL after the restoration of fucosylation contributes to the increase in tumor rejection caused by NK cell–mediated immune surveillance.

Aberrant Transcripts in Cancer Cell Lines and Somatic Mutations in Human Colon Cancer Tissues

To determine whether aberrant transcripts of *GMDS*, like those in HCT116 cells, are expressed in other cell lines, we performed RT-PCR analysis with RNA from an additional 10 colon cancer cell lines, including LS174T, SNUC4, SNUC5, C2A, HT29, HCT15, LoVo, SW948, NCI-H747, and NCI-H716. As a result, short transcripts were detected in two colon cancer cell lines, LS174T and NCI-H716 (Figure 5*A* and Supplementary Figure 1). Further sequencing analysis showed deletions of exons 2–4 and 5–7 of *GMDS* in the cDNA of LS174T and NCI-H716 cells, respectively. Transfection with a vector carrying each mutant *GMDS* into HCT116 cells caused no change of fucosylation (Figure 5*B*), indicating that the two mutant genes did not yield the enzymatic activity. However, expression of the WT *GMDS* protein and fucosylation were observed in these two cell lines because the cells expressed WT transcripts (Figure 5*A* and *C*). This finding indicates that these mutant *GMDS*s were not dominant-negative mutants. In a gastric choriocarcinoma cell line, SCH, a short transcript with deletion of exons 2–4 was found (Figure 5*D*). This cell line showed a marked decrease in the fucosylation level like HCT116 cells (Figure 5*E*). The transfection of WT *GMDS* into this cell line rescued cellular fucosylation, but those of other fucosylation-related genes such as FX, GDP-fucose transporter (GDP-fuc Tr), and α1-6 fucosyltransferase (FUT8) did not (Figure 5*F*). To examine whether genetic alterations of *GMDS* are involved in human carcinogenesis, we searched mutations of this gene in human colon cancer tissues. PCR and subsequent direct sequencing analysis identified mutations in 2 of 100 tumor tissues. One of the two was c.739 C>T (p.R247X) in exon 7, and the other was c.345+5 G>A (IVS4+5) in intron 4 (Supplementary Figure 2). These mutations were heterozygous, and no mutation was observed in the corresponding noncancerous tissues adjacent to the tumors, suggesting that the mutations were somatic events. As expected, the

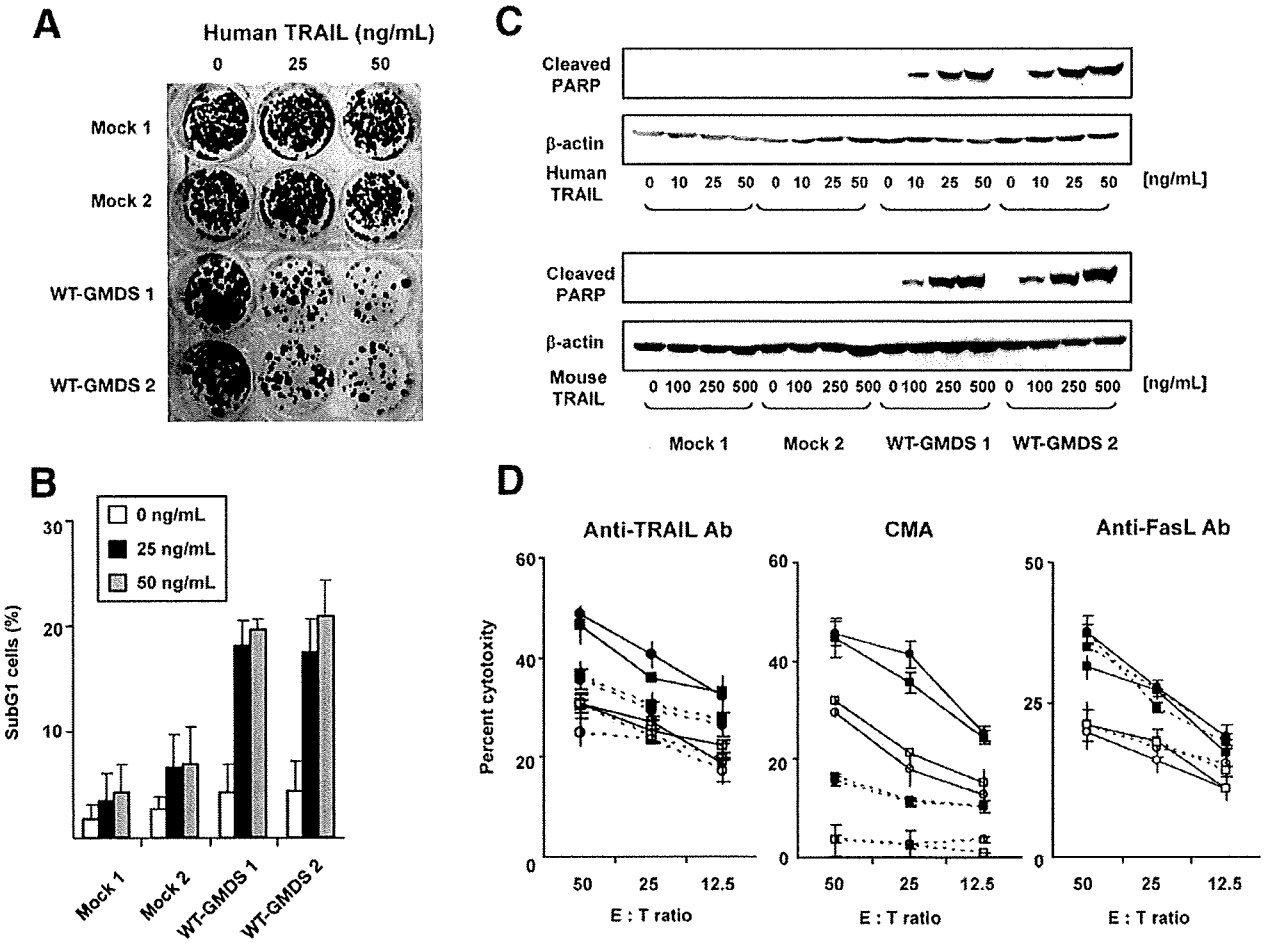

Figure 4. The effect on the susceptibility to TRAIL on the complementation of WT *GMDS*. (*A*) Clonogenic survival assay was performed. Detailed procedure is described in "Materials and Methods." (*B*) At 24 hours after the addition of TRAIL, the population of sub-G_1 cells was investigated with fluorescence-activated cell sorting. Data are represented as the ratio to total cells. *Bars* indicate SD. (*C*) At 2.5 hours after the addition of TRAIL, the expression level of cleaved PARP was determined by Western blotting. Western blotting of β-actin indicated that equal amounts of protein were loaded in each lane. (*D*) The effects of concanamycin A, anti-mouse Fas ligand, and anti-mouse TRAIL blocking antibody on the sensitivity of tumor cells to splenocytes was investigated by ^{51}Cr-releasing assay. *Open circles* indicate mock 1; *open squares*, mock 2; *filled circles*, WT-*GMDS* 1; and *filled squares*, WT-*GMDS* 2. *Bars* indicate SD. The *dotted lines* show the addition of concanamycin A, anti-mouse Fas ligand, or anti-mouse TRAIL blocking antibody.

nonsense mutation of c.739 C>T did not exhibit the enzymatic activity of *GMDS* (Figure 5*B*). The alterations of *GMDS* in the cell lines and colon cancer tissues are summarized in Table 2.

Discussion

Genomic instability is one of the hallmarks of cancer, in which an increased rate of genomic aberrations is directly involved in multistep carcinogenesis and cancer progression. The mutation identified in this study spontaneously arose in cells derived from human colon cancer. The suppression of tumor growth and metastasis in vivo on the complementation of the WT *GMDS* in *GMDS*-deficient cancer cells indicates that loss of function of *GMDS* facilitates cancer progression. Recently, it was reported that fucosylation was significantly higher in human colon cancers without lymph node metastasis than in ones with it, and higher in the early stage than in the advanced one.[17] The increases in fucosylation would be important at an early stage of carcinogenesis, and de-fucosylation would lead to cancer progression, including metastasis, which is a result of a dysfunction of the fucosylation pathway (Figure 6).

In this study, we have shown for the first time mutations of *GMDS* in human cancer. We first showed that HCT116 cells express aberrant *GMDS* transcripts. Although we searched mutations in the *GMDS* with DNA from the cells by PCR and direct sequencing, we did not find any mutations in the exons 4, 5, 6, 7, and 8 or their flanking intronic regions, suggesting that mutation in splice regulatory regions may not be involved in the generation of aberrant transcripts. Future identification

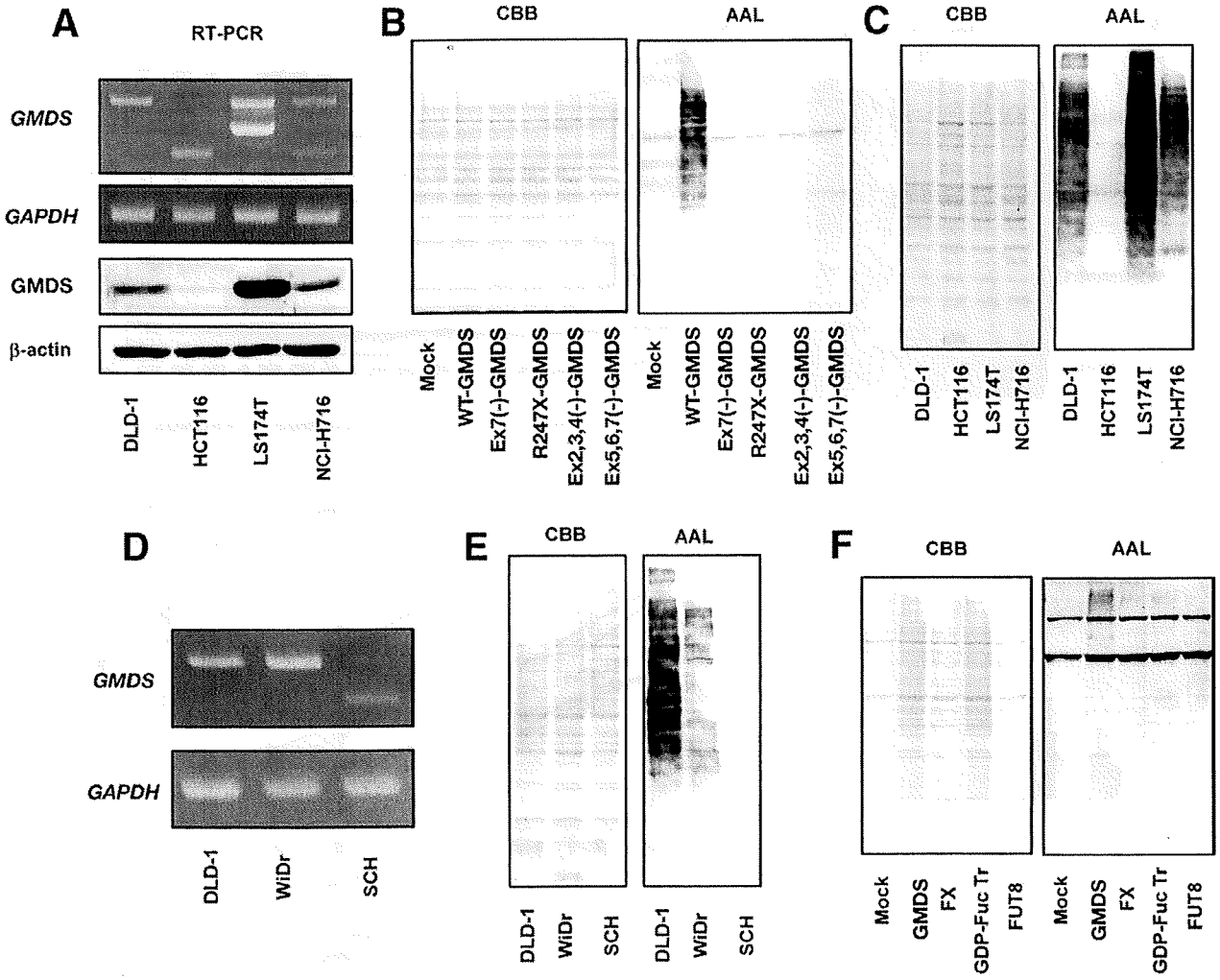

Figure 5. Additional mutations of the *GMDS* gene in cancer cell lines and tissues. (*A*) The expression patterns of *GMDS* in LS174T and NCI-H716 cells were investigated by RT-PCR and Western blot analysis. (*B*) After the expression vector carrying the WT or mutant *GMDS*, which were found in LS174T [Ex2,3,4(-)], NCI-H716 [Ex5,6,,7(-)], ovarian [Ex7(-)], and colon (R247X) cancer tissues, had been transfected into HCT116 cells, AAL blot analysis was performed. (*C*). The levels of fucosylation in these colon cancer cells were investigated by AAL blot analysis. (*D*) The expression pattern of *GMDS* mRNA in SCH cells was investigated by RT-PCR analysis. (*E*) AAL blot analysis of DLD-1, WiDr, and SCH cells. (*F*) After the expression vector carrying each fucosylation-related gene, *GMDS*, FX, GDP-fuc Tr, and FUT8, had been transfected into SCH cells, AAL blot analysis was performed.

of the breakpoint(s) will facilitate the understanding of mechanism of aberrant transcripts. Additional RT-PCR analysis unveiled that at least 3 of 13 colon cancer cell lines express aberrant transcripts. The mutant lines, LS174T and NCI-H716, expressed both mutant and WT transcripts. Taken together, loss of heterozygosity in *GMDS* may play a role in colon carcinogenesis. Our mutation search across the entire coding region of the *GMDS* identified two point mutations in colon cancer tissues. One of the two, a nonsense mutation of c.739 C>T, abolished enzymatic activity of *GMDS*. The other mutation (c.345+5 G>A) in the splice donor site of exon 4 has not been shown to lead deregulated splicing because RNA of the patient was unavailable. However, because G at the position of +5 in splice donor site is conserved and associates with U1snRNA in U2-type splicesomal complex, the substitution of G to A will be deleterious for the proper recognition by the complex.[33] Consistent with this view, all 3 computer algorithms for exon prediction, including NNSPLICE[34] (http://www.fruitfly.org/seq_tools/splice.html), NetGene2[35] (http://www.cbs.dtu.dk/services/NetGene2/), and Automated Splice Site Analysis[36] (https://splice.uwo.ca/), failed to predict the splice donor site with the mutant sequence, although they successfully predicted the natural donor site with the WT sequence (data not shown). Therefore, this mutation is likely to result in aberrant splicing such as exon 4 skipping or activation of cryptic splice site. In addition to the alteration in colon cancer cells, we showed that SCH cells expressed transcripts with a deletion of exons 2–4 in

Table 2. Status of the *GMDS* Gene in Cancer Cell Lines and Tissues[b]

Cell lines/tissues	Transcripts[a]	Genomic DNA	Classification
HCT116	Deletion of exons 5, 6, and 7	NA	Colon cancer cells
LS174T	Deletion of exons 2, 3, and 4	NA	Colon cancer cells
SNUC4	NAD	NA	Colon cancer cells
SNUC5	NAD	NA	Colon cancer cells
C2A	NAD	NA	Colon cancer cells
HT29	NAD	NA	Colon cancer cells
WiDr	NAD	NA	Colon cancer cells
HCT15	NAD	NA	Colon cancer cells
LoVo	NAD	NA	Colon cancer cells
DLD1	NAD	NA	Colon cancer cells
SW948	NAD	NA	Colon cancer cells
NCI-H747	NAD	NA	Colon cancer cells
NCI-H716	Deletion of exons 5, 6, and 7	NA	Colon cancer cells
SCH	Deletion of exons 2, 3, and 4	NA	Gastric choriocarcinoma cells
CRC79T	NA	c.345+5 G>A	Colon cancer tissue (T4, N2, M0)
LIN171T	NA	c.739 C>T	Colon cancer tissue (T2, NX, M0)

NOTE. NA, not analyzed; NAD, no abnormal transcripts detected.
[a]RT-PCR products were analyzed.
[b]Union Internatinale Contra la Cancer tumor-node-metastasis (TNM) stage is included in the parentheses.

GMDS, and that SCH cells were also resistant to TRAIL-induced apoptosis, like HCT116 cells (data not shown). Furthermore RT-PCR analysis identified aberrant transcripts in 5 of 10 microdissected ovarian cancer tissues (Supplementary Figure 3). The transcripts lacking exon 7 are assumed to truncate *GMDS* protein through the appearance of a stop codon in exon 8. This *GMDS* protein did not exhibit the enzymatic activity (Figure 5*B*). These data suggest that de-fucosylation as a result of *GMDS* mutation would be possible in other types of cancer, and that RT-PCR analysis is helpful for the evaluation of large deletions and splicing abnormalities. Although further studies are necessary to identify gross genetic alterations in ovarian cancer tissues as well as colon cancer tissues, alteration of *GMDS* transcripts should be involved in human carcinogenesis.

The gene encoding *GMDS* is located in chromosome region 6p25, in which a high LOH frequency was previously reported in invasive cervical cancer,[37] mantle cell lymphoma,[38] prostate cancer,[39] and ovarian cancer.[40] The two colon tumors harboring *GMDS* mutation were at advanced stages. Although we have not examined LOH in the tumors, inactivation of both *GMDS* alleles, a phenomenon of typical tumor suppressor genes representing

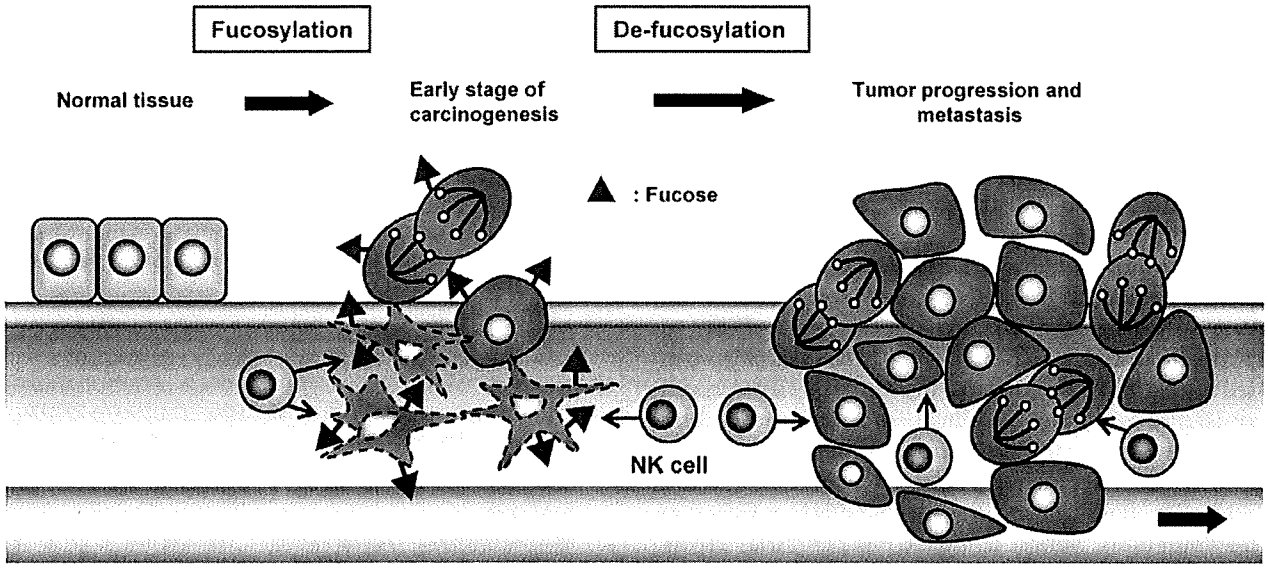

Figure 6. Schematic model of the biological functions of fucosylation and de-fucosylation in colon carcinogenesis. The level of fucosylation is not so high in normal colon tissues, but it is increased at an early stage of colon cancer. The cancer cells represented by the *dotted line* are apoptotic cells, which are attacked by NK cells. In certain types of advanced cancer, de-fucosylation through genetic mutation leads to escape from NK cell–mediated tumor surveillance and acquiring of more malignant characteristics.